

P-1690



Numerical Analysis of Combustion Process in Compression Ignition Engine



A Project Report

Submitted by

C.Baraneedharan - 71204402002

*in partial fulfillment for the award of the degree
of*

**Master of Engineering
in
CAD/CAM**



**DEPARTMENT OF MECHANICAL ENGINEERING
KUMARAGURU COLLEGE OF TECHNOLOGY
COIMBATORE - 641 006**

ANNA UNIVERSITY:: CHENNAI 600 025

ANNA UNIVERSITY:: CHENNAI 600 025

BONAFIDE CERTIFICATE

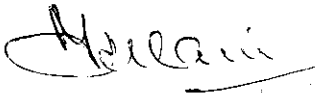
Certified that this project report entitled “Numerical Analysis of Combustion Process in Compression Ignition Engine” is the bonafide work of

Mr. C.Baraneedharan

-

Register No. 71204402002

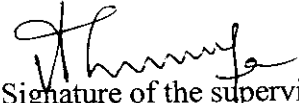
Who carried out the project work under my supervision.



Signature of the HOD

Dr. T. P. MANI

HEAD OF THE DEPARTMENT



Signature of the supervisor

Dr. V.VeL Murugan

ASSISTANT PROFESSOR

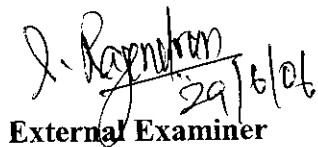


29/06/06

Internal Examiner

Dr. T.P. Mani

BE., M.E., PH.D., DML., MIE., MNOR., MISTE.,
Dean & HoD / Dept. of Mech. Engg.
Kumaraguru College of Technology
Coimbatore - 641 006



29/6/06

External Examiner

DEPARTMENT OF MECHANICAL ENGINEERING
KUMARAGURU COLLEGE OF TECHNOLOGY
COIMBATORE 641 006



BANNARIAMMAN
INSTITUTE OF TECHNOLOGY
Stay Ahead

National Conference on
Optimization Techniques in Engineering Sciences and Technologies

OPTEST - 2006



RMTUV

held at
BANNARIAMMAN INSTITUTE OF TECHNOLOGY

Sathyamangalam-638 401 during
April 11-12, 2006

Certificate

This is to certify that Mr./Ms./Mrs *C. Baraneedharan*.....
has participated / presented a paper entitled *NUMERICAL ANALYSIS OF THE COMBUSTION*

..... *PROCESS IN A COMPRESSION IGNITION ENGINE*.....

in the National Conference on "Optimization Techniques in Engineering Sciences and Technologies
(OPTEST-2006)" during 11-12 April 2006, organized by the Department of Mechanical Engineering,

Bannari Amman Institute of Technology, Sathyamangalam.

AG
C SASIKUMAR/ G SASIKUMAR
Organizing Secretaries

Dr K

Dr K THIRUNAVUKKARASU
Convener

Dr A
Dr A SHANMUGAM
Chairman

ABSTRACT

Intense competition and global regulations in the automotive industry has placed unprecedented demands on the performance, efficiency, and emissions of today's IC engines. The development of internal combustion engines requires the application of advanced tools. In addition to experimental methods, numerical simulation is needed to visualize the engine process. Therefore the sole objective of this project is to present the numerical simulation of flow, combustion and emission process in compression ignition engine.

To achieve this goal, a one dimensional combustion model with single-cylinder CI engine was first developed and investigations were performed. The numerical analysis were performed using the finite volume CFD code FLUENT. Simulation is done to analyze the turbulent intensity, production of kinetic energy. Combustion efficiency and exhaust gas composition more accurately. Eleven species were considered: O₂, CO₂, H₂O, N₂, H, O, N, H₂, OH, CO, and NO in emission. The boundary conditions for the simulation are ever gained by theoretical investigations.

The result obtained from the simulation is compared with the available theoretical values. The discussion reveals that during the combustion period the wall heat flux varies substantially in space and time, due to the transient nature of the flame propagation. The various emissions such as Carbon-monoxide, Carbon-dioxide, water, Nitrogen, Nitrous oxide are also predicted using the CFD code. Some of the emissions are compared with the theoretical chemical equilibrium. This emission in the exhaust valve shows large amount of NO_x which indicate that combustion is not at maximum efficiency.

ஆய்வு சுருக்கம்

இன்றைய வியாபார போட்டி மிகுந்த உலகினில் தானியங்கி வண்டிகளை தயாரிக்கும் தொழிற்சாலைகளும் தங்களது தயாரிப்புகளை உலக நடைமுறைகளுக்கு தகுந்தவாறு தர வேண்டிய கட்டாயத்தில் உள்ளன. இந்நிலையில் தானியங்கி துறையில் முக்கிய பங்கு வகிக்கும் உள் எரி எந்திர (IC Engine)த்தின், செயலாற்றும் விதம் செயல்திறன், வினை முடிந்து வெளியேற்றப்படும் பொருள்களின் தன்மை ஆகியவற்றை உலகளாவிய கட்டுப்பாட்டில் அமைய முயற்சிகள் மேற்கொள்ளப்படுகின்றது. இந்த பணிக்கு மேம்படுத்தப்பட்ட முறைகளை கையாண்டு புதிய ஆராய்ச்சி கருவிகள் மற்றும் எண் சார்பு பகர்வு போன்றவற்றை பயன்படுத்தி நன்முறையில் முடிவுகளை தர முயற்சிகள் மேற்கொள்ளப்படுகின்றது. எனவே இந்த ஆய்வின் நோக்கமானது உள் எரி எந்திரத்தின் செயல்திறன், செயலாற்றும் விதம் மற்றும் வினைமுடிந்து வெளியேற்றப்படும் வினை பொருட்களின் தன்மைகளை எண் சார்பு முறையில் கணினியின் உதவி கொண்டு கண்டறிதலாகும்.

இந்த ஆராய்வு ஒற்றை உருளை அழுத்த தீப்பற்று இயந்திரத்தில் மேற்கொள்ளப்பட்டது. Fluent மென்பொருளை உபயோகித்து எண் சார்பு ஆராய்ச்சி மேற்கொள்ளப்பட்டது. இந்த ஆராய்வானது வெளியேறும் வாயுவின் உட்பொருட்கள், உள் எரி எந்திரத்தின் பயனுறு திறன், கட்டுக்கடங்காத செறிவு மற்றும் இயக்க ஆற்றலின் உற்பத்தி ஆகியவற்றை ஆராய மேற்கொள்ளப்பட்டது. கணக்கில் எடுக்கப்பட்ட வினை பொருட்களாவன O_2 , CO_2 , H_2O , H , O , N , H_2 , OH , CO மற்றும் N_2 அறிமுறைசார் ஆராய்ச்சியில் இருந்து எல்லைக் காரணிகளானது பெறப்பட்டது.

இந்த ஆய்வின் விளைவானது அறிமுறைசார்பு மதிப்புடன் ஒப்பிடப்பட்டு சரிபார்க்கப்பட்டது. இந்த ஆராய்ச்சியிலிருந்து மாதிரியானது மேம்படுத்தப்பட்ட முடிவுகளை வெளிப்படுத்துகிறது.

ACKNOWLEDGEMENT

The author grateful to his guide **Dr.V.VeL Murugan**, Assistant Professor, Department of Mechanical Engineering, Kumaraguru College of Technology, Coimbatore for his excellent, utmost motivation, valuable advice, untiring support, timely suggestion, constant encouragement, enthusiasm, relentless patience, and inspiration throughout the study, holding in all the places.

The author expresses humble gratitude to **Dr.T.P.Mani**, Head of the Department, Mechanical Engineering, Kumaraguru College of Technology, Coimbatore for facilitating conditions for carrying out the work smoothly.

The author wish to express his deep sense of reverential gratitude to **Dr.K.K.Padmanabhan**, Principal, Kumaraguru College of Technology, Coimbatore, for providing the facilities to conduct this study.

The author expresses his heartfelt thanks to **Dr.N.Gunasekaran**, Professor, Department of Mechanical Engineering, Kumaraguru College of Technology, Coimbatore.

The author also wish to thank **Mr.B.N.Sriharan**, and **Mr.N.Siva Kumar**, Lab Technicians, CAD Lab for being with him throughout this venture, right from the scratch and helping for completing the project successfully.

The author owes his sincere thanks to all elders, parents, teachers and Lord Almighty who have bestowed upon their generous blessings in all endeavors.

CONTENT

Title	Page No.
Certificate	i
Abstract	iii
Acknowledgement	v
Contents	vi
List of Tables	ix
List of Figures	x
List of Symbols	xi

CHAPTER 1	INTRODUCTION	1
1.1	Introduction	2
1.2	Development IC Engine	2
1.3	Classification of IC Engine	3
1.4	Application of IC Engine	3
1.5	Compression Ignition Engine Operation	4
1.6	Motivation	7
CHAPTER 2	LITERATURE SURVEY	8
CHAPTER 3	DIRECT-INJECTION ENGINE COMBUSTION	11
3.1	Fuel Injection	12
3.2	Ignition Delay	13
3.3	Combustion Rates	16
3.3.1	Burning Rate Analysis	17
3.4	Chamber Geometry	21
3.5	Emissions	23
CHAPTER 4	TURBULENT FLOW AND MODEL	26
4.1	Turbulence Flow	27
4.2	Characteristics Of Turbulent Flow	28

4.3	Concept Of Eddy	29
4.4	Classification Of Turbulent Flow	30
4.5	Turbulence Modeling	30
4.6	Reynolds Time Averaging	31
4.7	Turbulence Parameters	32
4.8	Turbulence Model Equations	34
4.8.1	Turbulence Model	34
4.8.2	Spalart-Allmaras Turbulence Models	34
4.8.3	K-e Turbulence model	34
4.8.4	K-Omega Turbulence Model	35
4.8.5	Reynolds's Stress Equation Models	36
4.8.6	Recommendations	36
CHAPTER 5	COMPUTATIONAL FLUID DYNAMICS	37
5.1	Introduction	38
5.2	Governing Equation	39
5.3	Conservation of Mass	39
5.4	Conservation of Momentum	39
5.5	Energy Equation	40
5.6	Program Structure	40
5.7	Grid Generation and GAMBIT	41
5.8	Boundary Condition	45
5.9	Solution Algorithm	46
5.10	Convergence	47
5.11	Background on CFD Solver	47
5.12	CFD Modeling of diesel Engine	47
5.12.1	Grids and grid element equation	48
5.12.2	Spray Model	49
5.12.3	Ignition Model	50
5.12.4	Combustion	51
5.12.5	Emission Model	51

CHAPTER 6	MODELING OF IC ENGINE	53
6.1	Problem Definition	54
6.2	Geometry and Grid Generation	56
6.3	Boundary Condition	56
6.4	Pre-PDF Preprocessor	57
6.5	Setup and Solution	58
CHAPTER 7	RESULT AND DISCUSSION	60
CHAPTER 8	CONCLUSION	65
REFERENCES		68

LIST OF TABLES

Table	Title	Page No.
6.1	Engine General Specifications	54
6.2	Valve Timing Specification of DI Engine	54
6.3	Inlet valve specification of DI Engine	55
6.4	Exhaust Valve specification of DI Engine	55
6.5	The Injector Specification of DI Engine	55
6.6	Initial condition under point property	59

LIST OF FIGURES

Figure No.	Title	Page No.
1.1	Four Stroke of the 4-Stroke Engine	5
1.2	P-V diagram of a four stroke diesel engine	6
3.1	Diagram of Diesel combustion processes	14
3.2	Total and radiant heat flux	19
3.3	Combustion chamber configurations	22
3.4	Comparison of Engine Performance between Flat Dish and HMMS	23
3.5	Comparison of Calculated and Experimental Nitric Oxide	24
5.1	Basic Flow Structure	40
5.2	Union of cube, a cylinder, and a triangular prism	44
5.3	Cooper meshing scheme	44
5.4	Computational Mesh for Simulation of Engine	49
5.5	Crank angle Vs NO _x and soot	52
6.1	Model and Grid Generation	56
6.2	Various Components in the Model	57
6.3	Chemical Species	57
6.4	Mesh Motion	58
7.1	Mass Fraction of Burned at Starting of Suction Stroke	61
7.2	Mass Fraction Of Burned At Angle of 430°	61
7.3	Turbulence Kinetic Energy	62
7.4	Mass Fraction Of Burned At Starting Of Exhaust Stroke	62
7.5	Mole Concentration of CO	63
7.6	Mole Concentration of CO ₂	63
7.7	Mole Concentration of H ₂	64
7.8	Mole Concentration of N ₂	64

LIST OF SYMBOLS

T	mass average gas temperature, K
T_w	Temperature of surface area A, K
\bar{h}	$0.82d^{-0.2} W^{0.8} T^{-0.53}$, $\text{kw/m}^2 \cdot \text{K}$
p	Cylinder pressure, MPa
d	Cylinder bore, m
q_c	Constant energy rate
q_L	Heat transfer rate
\bar{U}	Instantaneous Velocity
U'	Turbulence Intensity
ρ	Density
\vec{V}	Vector velocity of fluid
P_1, V_1, T_1	Reference value at intake valve
P_o	Cylinder gas pressure, MPa
C_m	Mean piston speed, m/s
V_d	Displacement volume, m^3
R^*	Generic radical pool
Q	Intermediate species
B	Branching agent

Chapter 1

Introduction

1.1 INTRODUCTION

The function of internal combustion engine is to produce mechanical power from chemical energy contained in fuel. The air – fuel mixture before combustion and products of desired power output, occurs directly between these fluids and the mechanical components of the engine. Because of the simplicity, ruggedness and high power to weight ratio, these engines have found wide application in transportation and power generation. It is a fact that combustion takes place inside the cylinder of the engine that makes the design and operating characteristics fundamentally from that of the open and closed combustion system.

An internal combustion engine offers the following advantages over external combustion engine

1. Overall efficiency is high
2. Greater mechanical simplicity
3. Weight to power ratio is generally low
4. Generally lower initial cost
5. These units are compact and thus requires less space

1.2 DEVELOPMENT OF I.C ENGINE

Many experimental engines were constructed around 1878. The first really successful engine did not appear, however until 1879, when a German engineer Dr.Otto built his famous Otto gas engine. The operating cycle of this engine was based upon principles first laid down in 1860 by a French engineer named Bea de Rochas. The majority of modern I.C engine operate according to these principles.

The development of the well known diesel engine began about 1833 by rudoff Diesel. Although this differs in many important respects from the Otto engine, the operating cycle of modern high speed diesel engine engines is thermodynamically very similar to Otto cycle.

1.3 CLASSIFICATION OF IC ENGINE

Major classification of Internal Combustion engine are given below

1. According to cycle of operation
 - Two stroke cycle engines
 - Four stroke cycle engine

2. According to method of ignition
 - Spark ignition engine
 - Compression ignition engine

3. According to cycle of combustion
 - Otto cycle engine
 - Diesel cycle engine
 - Dual cycle engine

1.4 APPLICATION OF I.C ENGINE

The I.C engine are generally used for

- Road vehicles
- Air craft
- Locomotives
- Pumping sets
- Cinemas
- Hospital
- Construction in civil engineering equipment
- Several industrial application

1.5 COMPRESSION IGNITION ENGINE OPERATION

In compression ignition engine, air is drawn into the cylinder. The fuel is injected directly into the cylinder just before the piston reaches the top dead centre (i.e.) just before the combustion starts. Varying the amount of fuel injected makes load control in each cycle, the airflow at the given engine, the compression ratio of the engine is much higher than that of the spark ignition engine, the compression ignition engine have compression ratio in the range of 12 to 24, depending upon the type of diesel engine and whether the engine is naturally aspirated or turbocharged. Air at atmospheric pressure is drawn during the suction stroke and then compressed to a pressure of about 4 MPa and temperature of about 800K during the compression stroke.

At about 20° before top dead center, fuel injection into the cylinder commences, the fuel is injected into the cylinder in the form of a fine spray and the atomized fuel vapor then mixes with the air to the combustible proportions. The temperature and pressure of the air are above the fuel ignition point. Therefore after a short delay, spontaneous ignition of parts of the non-uniform fuel air mixture initiates the combustion process, and the cylinder pressure rises above the non-firing engine level. The flame spreads rapidly throughout the portion of the sufficiently mixed air-fuel mixture, the expansion process proceeds. At full load, the mass of fuel injected is about 5% of the mass of air in cylinder, increasing levels of smoke in the exhaust stroke, gases are pushed out, but some remain in cylinder as residual gas.

In this project, the four-stroke compression ignition engine working on diesel is chosen. The operation is based on the diesel cycle. The air is sucked at constant pressure, the sucked air undergoes compression in isentropic process, heat addition is at constant pressure process and expansion takes place in isentropic processes, the exhaust process takes place at constant volume process.

The various stroke of four stroke (diesel) cycle engine are detailed in the figure 1.1.

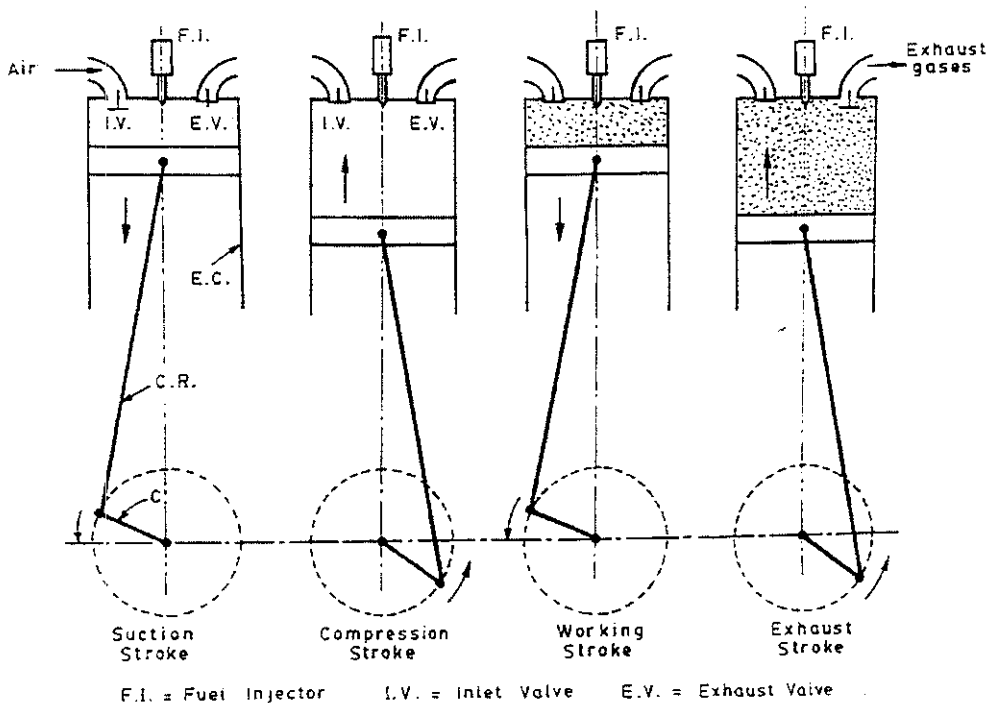


FIG 1.1 FOUR STROKE OF THE 4-STROKE ENGINE

1. Suction Stroke

With the movement of the piston from T.D.C to B.D.C, during this stroke, the inlet valve opens and the air at atmospheric pressure is drawn inside the engine cylinder. The exhaust valve however remains closed. This operation is represented by line 5-1 in the figure 1.2.

2. Compression Stroke

The air drawn at atmospheric pressure during the suction stroke is compressed to high pressure and temperature (to the value of 35 bar and 600 C respectively) as the piston moves from B.D.C to T.D.C. this operation is represented by 1-2. Both the inlet and exhaust valves do not open during any part of this stroke.

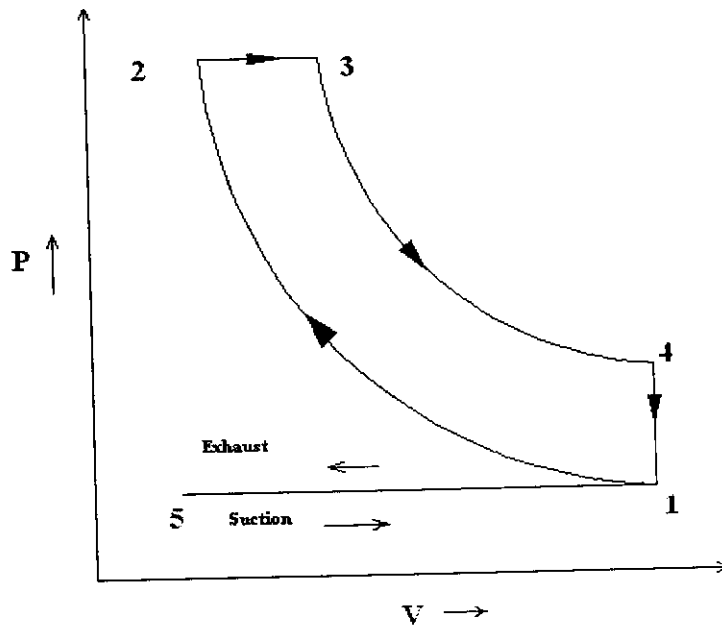


FIG 1.2 P-V DIAGRAM OF A FOUR STROKE DIESEL ENGINE

3. Expansion or Working Stroke

As the piston starts moving from T.D.C. a mattered quantity of fuel is injected into the hot compressed air in fine spray by the fuel injector and it (fuel) starts burning at constant pressure as shown by the line 2-3, at the point 3 fuel supply is cut-off. The fuel is injected at the end of compression stroke but in actual practice the ignition of fuel starts before the end of the compression stroke. The hot gasses of the cylinder expand adiabatically to point 4, thus doing work on the piston. The expansion is shown by 3-4.

4. Exhaust Stroke

The piston moves from the B.D.C to T.D.C and the exhaust gasses escape to the atmosphere through the exhaust valve. When the piston reaches the T.D.C the exhaust valve closes and the cycle is completed. This stroke is represented by line 1-5

1.6 MOTIVATION

The recent increase in computing power coupled with the declining cost of computers has led to a rapid development in the science of computational fluid dynamics (CFD) simulation. Simulation can be defined as the prediction and reconstruction of behaviour of a product or physical situation under assumed or known conditions. It is widely used in various engineering disciplines as a means of quickly determining or improving the behaviour of a design, thus saving on experimental work that can be expensive.

However, the emergence of simulation has not made experimental tests obsolete, as these are important for verification during the design process. CFD as a simulation tool has proved itself to be extremely useful over the years, especially since some phenomena cannot be determined experimentally. It has also been successfully used in the aerospace industry to predict aerodynamic behaviour of aircraft components such as wings, canards, etc. These simulations also yield derived flow information such as vorticity and residence time, which are difficult to measure. CFD has also been extended for use in industrial applications such as continuous steel casting and automotive engine cooling.

The use of CFD in prediction and improvement of system behaviour has, over the years, gained acceptance in industrial application. This approach has worked well in the improvement of an automobile combustion system, where the results were also validated. Achieving improvement without going the trial-and-error route is essential for economy and time reasons, which is the reason that CFD and mathematical optimization were employed in this endeavour. Also, previous experimental attempts to improve the combustion system that is the subject of this study have yielded little success, hence the decision to use numerical techniques.

The sole objective of this study is to determine and improve the engine flow and combustion system of the concerned engine through the use of the combination of CFD. Understandably, the accuracy of numerical methods is of great concern especially in CFD with the wide choice of modeling options, all which give converged but different solutions.

Chapter 2

Literature Review

Holger Peters, Ulrich Spicher (2001). The investigations were performed in a 6-cylinder CI engine running at wide open. Combustion in the present study was treated with the one-equation flame let model. This model was implemented in FLUENT. This mass fraction of the combustion products was assumed to follow the local and instantaneous thermodynamic equilibrium values. The equilibrium composition of the cylinder charge was calculated. Eleven species were considered: O₂, CO₂, H₂O, N₂, H, O, N, H₂, OH, CO, and NO. Isooctane was used as fuel. For the calculation of the convective heat transfer during the combustion process a further sub model for the calculation of the heat transfer coefficient was used.

Mayer, Spicher, (2000). This study is concerned with the CFD prediction of wall heat transfer in reciprocating engines, with particular reference to Diesel engines working at high peak pressures. To this end, CFD simulations are performed of flow, combustion and heat transfer in prototype Diesel engine for which detailed local time-resolved surface heat transfer measurements have been performed. Comparisons are made between these data and predictions based on two wall heat transfer treatments, one of which ignores the effects of variations of thermo physical properties and another which takes them into account. The latter treatment is shown to produce substantially better agreement than the former. Finally, it is shown that local heat transfer measurements also provide a stringent testing ground for spray and combustion model performance.

Sangjin Hong, Dennis Assanis, Margaret Wooldridge (2003). This study was conducted to predict the emission of pollutants such as soot and nitrogen oxide (NO) more accurately and to enhance understanding of the pollutant formation process. To achieve this goal, a combustion model was first developed. It was based on the fact that the reaction rate during combustion was determined by the interaction between the chemical reaction rate and mixing rate. In a cylinder chamber, soot particles are affected by the flow motion but their transport characteristics are different from other species. Soot formation and destruction rates can be predicted more accurately with spatial distribution of soot particles.

R.Payri, B.Tormos, F.J.Salvador (2005). A combined experimental and computational investigation was performed in order to evaluate the influence of nozzle geometry on fuel injection rate and the injector dynamic of a common-rail fuel injection system for DI diesel engines. A series of parametric studies were performed to evaluate the influence of the nozzle seat type and the nozzle orifice geometry. Experimental results of the fuel injection rate were included to validate the models.

Trigui (1999) has presented the details that intense competition and global regulation in the automotive industry has placed unprecedented demands on the performance, efficiency, and emission of today's IC engines. It reduces the making of prototype cost and simulation of gas cycle motion inside the cylinder. It shows the methodology to optimize the IC engine design for the future technology.

Chapter 3

*Direct-injection engine
combustion*

3.1 FUEL INJECTION

The primary purpose of the injector is to distribute and mix the fuel with the surrounding air. Because the engine load is controlled by the amount of fuel injected, the injector must handle a volume of fuel which ranges over an order of magnitude. The maximum fuel/air ratio is determined by the allowable smoke level and is typically at 0.8 equivalence ratio for an NA engine.

For a fixed injection pressure, the amount of fuel injected is changed by changing the injection duration. The injection duration for a fixed pressure and amount of fuel per cylinder can be increased by decreasing the hole size or number of holes in the injector tip. Hole size is limited by the method of fabrication, which utilizes either small drills or electro discharge machining. Holes of 0.2 mm diameter are routinely obtained with good reproducible quality. Holes down to 0.1 mm (0.004 in.) can be fabricated, but quality control is a problem. Even very small imperfections will cause quite significant changes in the spray pattern. Even a 1° change in angle between spray axis and head or a few millimeters change in injection tip depth can cause serious problems. In order to provide minimum breakup length, the length-to-diameter ratio of the holes should be kept in the 3-5 range. Of course, each hole should have the same flow coefficient. Thus, testing of the injector by spraying into open air or into a see-through chamber containing nitrogen gas or kerosene is typically employed as a means of inspection. Measurement of the volume of fuel injected by each hole is also advisable. It is also important that each cylinder receive the same injection, especially from an emissions standpoint.

The spray formulas were developed for non vaporizing cases. A comparison of penetration with and without vaporization and/or combustion from experiments carried out in a rapid compression machine and in a constant volume bomb shows decreases in penetration of only 10-20% due to vaporization; however, the important factor should be the overall effect on fuel distribution. One must also be careful to note that the spray momentum and droplet size distribution greatly confound this result. Recall that the liquid penetration is caused by newly formed drops overtaking and passing previously formed drops. Thus, the drops

MPa) sprays with small nozzle holes (0.1 mm), the droplets are very small and thus the spray vaporizes rapidly, giving a gas-jet- like behaviour.

Laser sheet diagnostics indicate that at full load the spray becomes vaporized less than one inch from the nozzle. Although the jet will penetrate well, its ability to mix rapidly may be less than would be expected from previous experience with less vaporized sprays. However, the high momentum of such high-pressure sprays increases mixing greatly compared with lower pressure sprays. For heavy-duty engines, liquid impingement on the piston bowl surface should not be a problem for such sprays except during cold starting.

In small high speed diesels the liquid fuel impinges on the piston bowl surface because of the small bore. Swirl can be used to shorten the penetration and improve mixing. But typically at a cost in terms of reduced volumetric efficiency and increased heat transfer. Droplets reaching the surface may wet the surface or rebound. For many conditions, rebounding also results in droplet break up. Detailed models involving all of these effects as well as heat transfer are currently being developed and evaluated for use in CFD codes.

3.2 IGNITION DELAY

Recall that the time (or crank degrees) between the start of injection and the start of combustion is called the ignition delay. During the delay period, fuel is continuously injected and vaporized for open chamber engines, the effect of injection pressure, Nozzle hole diameter, and number of holes seems to have only a minor influence on the delay period. This is particularly true for turbo charged engines. Thus the delay is primarily a function of those parameters which affect the chemical reaction rate of the fuel vapour mixtures. This fact is counterintuitive, since the liquid fuel must be disintegrated into droplets, vaporized, and mixed with air before significant reactions can take place.

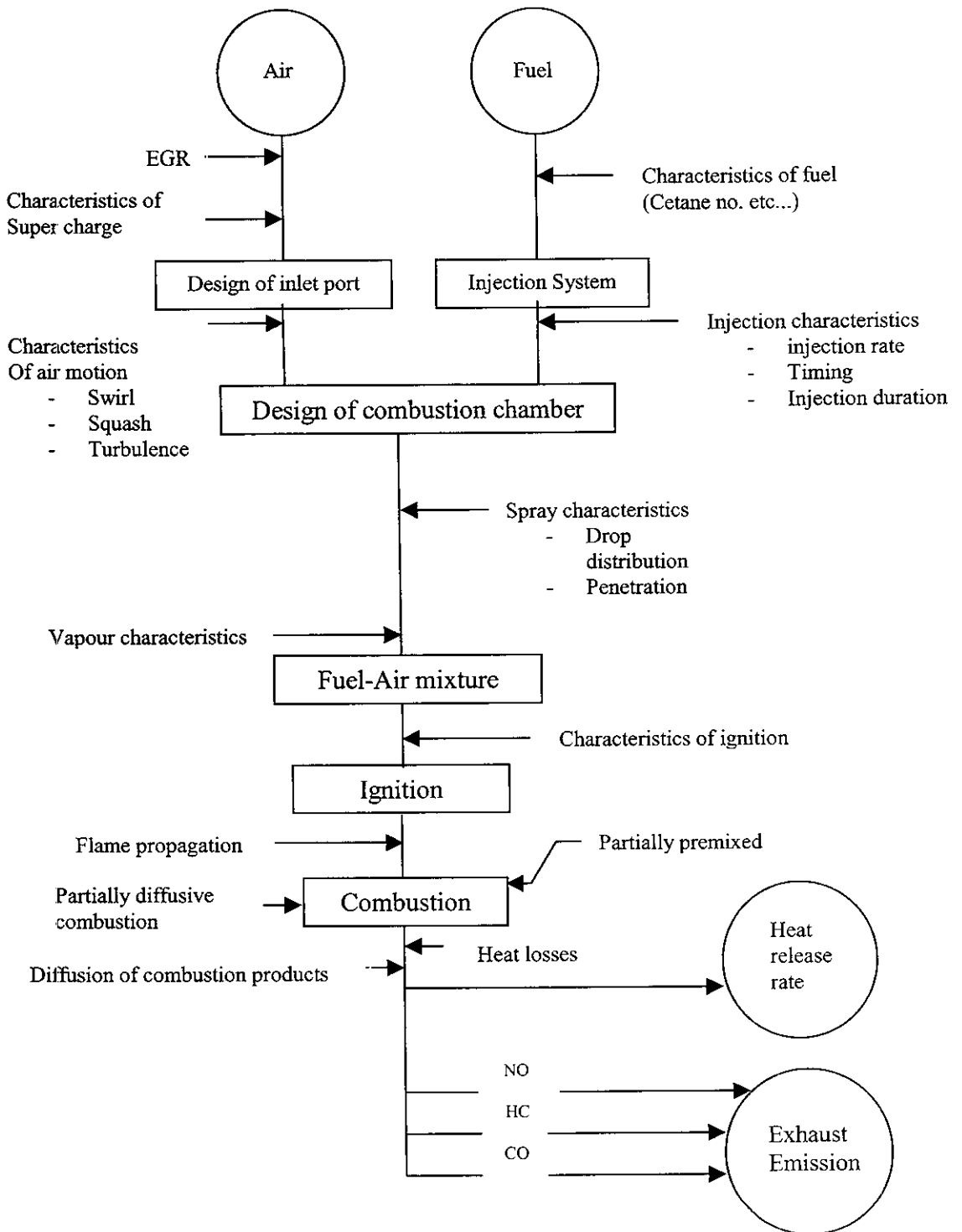


FIG 3.1 DIAGRAM OF DIESEL COMBUSTION PROCESSES

However, it appears that the physical delay due to this process is not controlling. One explanation is that a small amount of appropriate fuel / air mixture is always

delay are more important in pre chamber (IDI) engines, where fuel atomization and mixing are less rapid. Similarly, constant – volume combustion bombs, often used for experiments on ignition delay, typically have longer delay periods due to lower pressures, temperatures, and turbulence in the bomb than in engines.

The major reason that long ignition delays are not tolerated is that a large amount of fuel vaporizes and mixes with air prior to ignition if the delay is long. When ignition takes place, this prepared fuel burns rapidly, giving a high rate of pressure rise, a high peak pressure, and a characteristic sharp knocking sound. Continued operation at such conditions can cause mechanical failure due to head gasket failures or to main bearing failures, and / or failure to meet noise control standards. Retarding the injection timing, recalculating some exhaust gas, or heating the inlet air may help, but may also produce undesirable changes in performance and / or emissions. Design changes to reduce these problems will be discussed later, but for now it is clear that ignition delay can be a limiting factor in diesel engine performance.

Formulas for prediction of ignition delay have been obtained from both engine and bomb test. The independent variables are typically average cylinder gas pressure during the delay, average cylinder gas temperature during the delay, fuel cetane number, and engine fuel /air ratio. The most important variable is temperature; however recent tests in a bomb have indicated that at temperatures above 800 K (10000 F) the effect of temperature isles significant. This indicates that if the chemical kinetic delay is very short, the physical delay may be to play a role. however, engine experiments with a small amount of fuel burned prior to main injection have obtained delays smaller than 1 CA⁰ at speeds of 2000 rpm (about 80us) indicating that the physical preparation time is quite small.

A typical correlation formula is of the form.

$$\Delta t = C \left(\frac{P}{P_0} \right)^a (F)^b \exp \left(\frac{E}{RT} \right) \quad (3.1)$$

Where the constant E depends on the fuel formulation $-1.9 < a < -0.8$, $-1.09 < b < -1.6$, and P_0 is a reference pressure. The constant C depends on the engine. Inclusion of the equivalence ratio is not always necessary.

Before leaving this discussion of ignition delay it may be useful to comment on the chemical kinetics during the delay process. Experiments with pilot injection have shown that even very low - Cetane fuels can be ignited in a warm engine if the pilot fuel do not release much energy, indicating that the reactions have not yet produced significant.

Modeling with CFD allows use of simplified ignition models such as the shell model originally developed for knocking reactions in S.I. engines. This model contains 33 empirical constants which depend

3.3 COMBUSTION RATES

The amount of mixtures which burns rapidly following ignition is determined by the fuel properties, the injection parameters, the flow pattern in the cylinder, the temperature and pressure of the cylinder's gas, and the ignition delay. Following this rapid (premixed) burning, the combustion rate is controlled by mixing rates for most engines under fully warmed up conditions. Calculation based on spray models indicate that vaporization of droplets is not rate-controlling unless the engine is cold and / or the spray is very coarse. Modern turbocharged engines with high injection pressures the vaporization rate is unlikely to control the rate of combustion except under cold starting conditions.

Unfortunately, mixing models for sprays under the three-dimensional turbulent flow conditions encountered in engines have not been validated. It must be recognized that although vaporization is not rate-controlling, it does profoundly affect the fuel/air ratio distribution. Furthermore, the spray penetration determines the amount of fuel which interacts with the piston bowl surfaces. Given this modeling difficulty, it is not yet possible to predict diesel design configurations or even combustion trends from fundamental models based on first principles. Recently, however, the application of detailed CFD modeling has shown the ability to reproduce the burning rates obtained from pressure data. This is

applied to a wide range of engines and conditions, so one cannot say yet that the CFD models are reliable for design purposes. As a result, the most common approach is to obtain the burning rate from analysis of cylinder pressure data. If enough data are taken for a given engine family (a series of engines of various sizes, but all with the same design philosophy), it is possible to correlate the burning rate data using empirical or quasi-empirical formulas.

Attempts to obtain predictive models by semi empirical modeling (so-called phenomenological models, which use approximate equations containing many adjustable constants) have sometimes given good results when properly tuned using data, but have not shown the ability to be predictive without such empirical adjustments. Thus we shall give only a heuristic discussion of such models and focus most of our attention on pressure data analysis, which gives an apparent rate of burning.

3.3.1 Burning Rate Analysis

The rate of combustion can be determined from analysis of cylinder pressure if one assumes that the pressure is uniform so that the measured pressure is the pressure acting on the piston surface. The integral of $p \, dV$ thus gives the work done over the interval of integration. As a first step, consider the combustion to act as uniform energy rate addition q_c , neglect all changes in composition, and assume constant specific heats. Then the energy equation for this single-zone model is

$$mc_v \frac{dT}{dt} + p \frac{dV}{dt} = q_c - q_l = q_{(net)} \quad (3.2)$$

The quantity $q_{(net)}$ is the energy rate addition due to combustion less the heat transfer rate q_l out through the chamber surfaces. From the ideal gas equation, neglecting the change in the gas mass due to vaporization of liquid fuel,

$$q_{(net)} = p \frac{dV}{dt} + \frac{p \frac{dV}{dt} + V \frac{dp}{dt}}{\gamma - 1} \quad (3.3)$$

Integrating with γ constant,

$$Q_{(net)} = \int_{\theta_1}^{\theta_2} q_{(net)} \left(\frac{dt}{d\theta} \right) d\theta = \int_{v_1}^{v_2} p dV + \frac{(pV)_2 - (pV)_1}{\gamma - 1} \quad (3.4)$$

The right side of the above equation is evaluated from values of $V(\theta)$, $p(\theta)$, and $p(\theta)$ obtained from the cylinder pressure data. It must be warned, however, that obtaining good pressure data is not easy. To obtain reasonable pressure data the crank angle interval of sampling must be at least 0.5 crank degrees or, better, 0.1 crank-degrees. Proper filtering of the typically necessary to ensemble-average the data over at least 100 cycles in order to remove noise and average random cyclic variations.

The simple heat release rate of Eq. 3.3 or the integrated value of Eq. 3.4 above contains the confounding heat transfer; q_l . Accurate evaluation of q_l is not possible from current theory. During the mixing-controlled combustion, the flame is quite luminous due to the formation of carbon particulate. These tiny particles, which are a fraction of a micron in size, each radiate as essentially black bodies. In older engines the resulting flux of radiation gave a peak value about equal to the peak convective flux. Modeling of this flux could be done in detail if the spatial distribution of carbon and its temperature were known. However, the distributions are not known, and thus only approximate representations can be given. Modern low shooting engines have much reduced radiation components. Recent data indicate that the peak radiation flux is only 30% of the total flux and that radiation accounts for only 15% of the total heat transfer to the combustion chamber surfaces.

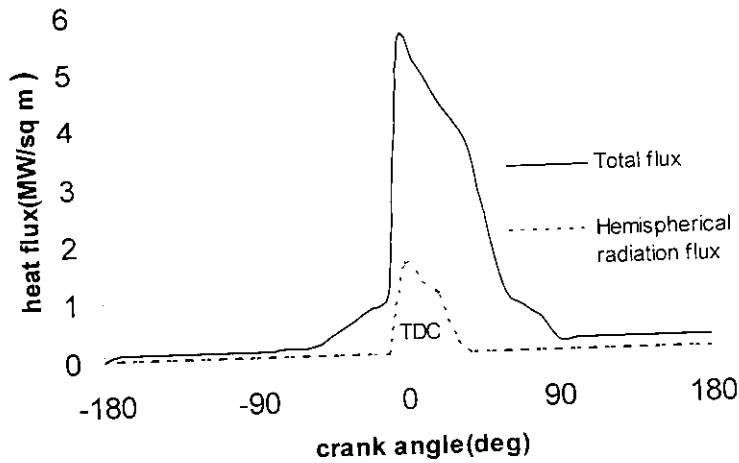


FIG 3.2 TOTAL AND RADIANT HEAT FLUX

The Figure 3.2 shows histories of total and radiations flux measured on the head of fired turbocharged diesel. The convective flux measurement during combustion is confounded by the more difficult-to-measure radiation. In addition, measurements have shown that the total heat flux (radiation plus convection) is very non- uniformly distributed. At the present time only approximate correlations are available, and the most widely used is due to Woschni. This formula laniaries the radiation term and combines it with the convective term to give

$$q_L = \bar{h}A(T - T_w) \quad (3.5)$$

In order to calibrate such formula it is necessary to apply an energy balance between the start of injection and beyond the end of combustion. To be on the safe side it may be necessary to assume combustion ends at exhaust valve closing. The first law, with the internal energy of formation included in u and h_f , may be written as

$${}_1Q_2 = - \int_{v_1}^{v_2} pdV - (m_2u_2 - m_1u_1) + h_f(m_2 - m_1) \quad (3.6)$$

Step-by-step integration of q_L , using the Eq. 3.5 with $T=pV/mR$ will give $C=1$ in Eq. 3.6 if the equation for h is correct. In practice C can be quite different

the total global value, ${}_1Q_2$, to balance the energy, but this does not mean that the shape of q_L versus θ is correct. In fact, it is known from experiment that local values of q_L can change sign during the period 55-65 crank degrees after TDC even though $T > T_w$ during that period. The reason for this is shown by theory to be the expansion of the cool boundary layer gases to below the wall temperature, which the hot bulk gas, although also cooled by expansion, is still at a much higher temperature than the wall.

The temperature calculated for a motored engine using a multidimensional model for the gas and the law of the wall for the boundary layer profiles. One can see the minimum in the temperature profile for the 40CA' curve during expansion. The empirical Eq. 3.5 is based on the mass average temperature and thus always predicts that the heat flux is from the gas to the wall when the mass-averaged gas temperature is higher than the wall temperature. The fact that both q_c and q_L are small at the same time and q_L is not well known means that it is very difficult to determine the exact end of burning.

To solve the Eq. 3.2 the gas phase is modeled as air. Of course, the gas phase is heterogeneous system of hot products, air, fuel vapour mixed with air, and liquid fuel. The question then becomes how to more accurately model the internal energy term in the first law rate equation. A simple one zone model, although inaccurate, is often used. In this model the fuel vapor and liquid parts of the system are ignored and the air products are taken as perfectly mixed. The model starts with air-residual mixture and assumes that fuel is introduced to the system at a rate just equal to the burning rate. The system equivalence ratio thus starts near zero and grows to the final overall engine value. Because hot rich zones are neglected in this model, the effects of dissociation are very small. A term must be introduced for the addition of the fuel enthalpy, hf . The internal energy is for products and now includes the chemical energy:

$$\frac{du}{dt} = \left(\frac{\partial u}{\partial T} \right) \frac{dT}{dt} + \left(\frac{\partial u}{\partial F} \right) \frac{dF}{dt} \quad (3.7)$$

Introduction of a heat transfer model, the ideal gas equation, and measure pressure data allows solution for m_f and T as functions of crank angle or time. In this model, m_f is an apparent fuel burning rate (AFBR).

More recently the model of Hiroyasu has offered a compromise between CFD modeling on supercomputers and a gas jet model such as provided by the Cummins model. The Hiroyasu model, which can be run on a personal computer, uses a crude grid and a spray droplet model. Because the grid is crude, the model depends strongly on semi empirical sub grid models. Such models can be tuned to a particular engine and then used for guidance in design, but are unlikely to predict correctly without tuning by use of engine-specific data.

3.4 CHAMBER GEOMETRY

Thus far the discussion of diesel combustion has centered on the spray characteristics. However, the shape of the combustion chamber and the fluid motion in it are also of importance. The characteristics of the flow at time of injection are determined by the inlet port and valve configuration, and the chamber shape. The major effect of the intake process is to determine the large-scale motions in the chamber at intake valve closing. As the piston moves upward, the gas is pushed into the piston bowl. If the gas is swirling, the swirl will increase due to conservation of angular momentum. Recall that the radial inward velocity of the flow caused by the piston motion is called the squish velocity. Although the direct effects of the squish velocity are probably small, the indirect effects on the motion in the bowl can be quite significant. The shape of the edge of the bowl is also important. A reentrant shape may set up vertical vortices in the bowl and can greatly influence the way the combustion products leave the bowl during the expansion stroke; this outflow is sometimes called reverse squish.

Swirl has a profound influence on mixing between the fuel plumes and the air during the injection period. After the end of injection the primary contribution of swirl is through its decay to turbulent motion. The swirl also tends to stabilize the flow, reducing cycle-to-cycle flow variations. Chambers with low swirl tend to have tumbling vortices which can shift from one cycle to the next. But the more

of high swirl are to cause the hot, less dense products to move to the center of the chamber, thus reducing mixing, to cause reduction in spray penetration, to produce lean mixtures which do not burn or only partially burn, thus causing unburned hydrocarbon and CO exhaust emissions; to increase heat transfer; and to increase the premixed burn fraction.

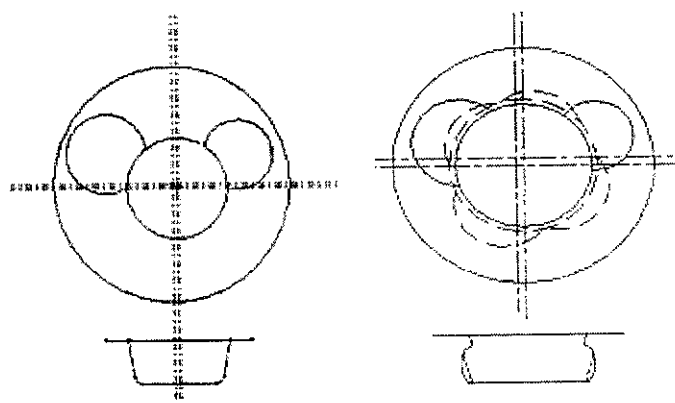


**FIG 3.3 COMBUSTION CHAMBER CONFIGURATIONS-
FLAT DISC AND HMMS**

Low-swirl engines with shallow, wide bowl combustion chambers and high injection pressures need to have nozzles with many holes (8-10) to compensate for the lack of tangential mixing that would be caused by swirl. Such chambers typically lack mixing during the later part of the combustion period. Unique designs of the chamber shape may provide a solution to these problems. figure 3.3 shows three chamber shapes. The odd pocket shapes of the Hino Motors Micro Mixing System (HMMS) cause some of the swirl to be converted to vortices in each pocket during the expansion stroke. This system also seems to increase the higher-frequency components of the turbulent energy. The increased mixing after TDC results in improved performance and emissions as shown in figure 3.4. A flat dish design gave more premixed burning and more late combustion than the HMMS design.

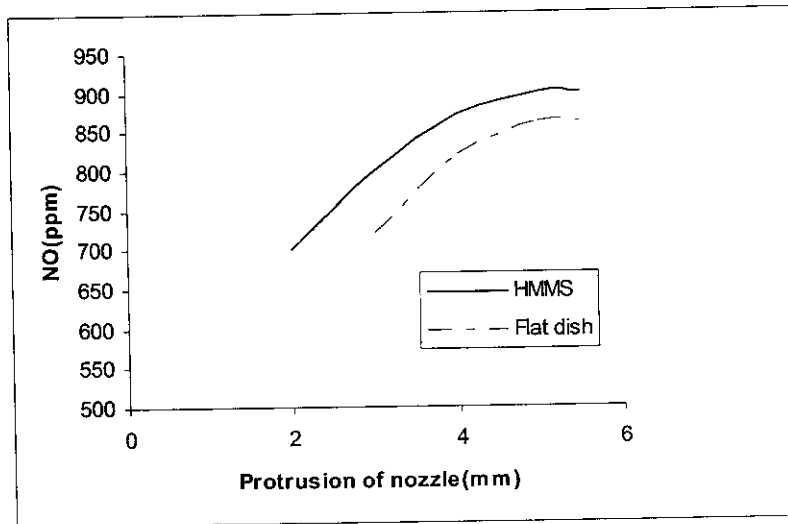


FIG 3.4 COMPARISON OF ENGINE PERFORMANCE BETWEEN FLAT DISH AND HMMS

3.5 EMISSIONS

The two most troublesome emissions from diesel engines are soot (particulates) and nitrogen oxides) typically, unburned hydro carbons and CO are not a serious problem except at light loads. Hydrocarbons can arise from fuel is less apt to impinge on surfaces, but because of poor fuel distribution, large amounts of excess air, and low exhaust temperature, lean fuel-air mixture regions may survive to escape into the exhaust. White smoke is often observed at low load conditions and is really a fuel particulate fog.

The more typical black smoke sometimes observed during periods of rapid load increase, or for older engines at higher loads, is made up primarily of carbon particles. At higher loads the higher temperatures tend to oxidize even lean mixtures. In homogeneous charge automobile engines, unburned hydrocarbon emissions are high during startup, when the catalyst is too cold to be effective. Diesels provide reduced hydrocarbons in automobiles even though they have no catalyst system. This is only true, of course, if the diesel starts promptly, and thus starting aids such as glow plugs are often used in automotive diesel applications.

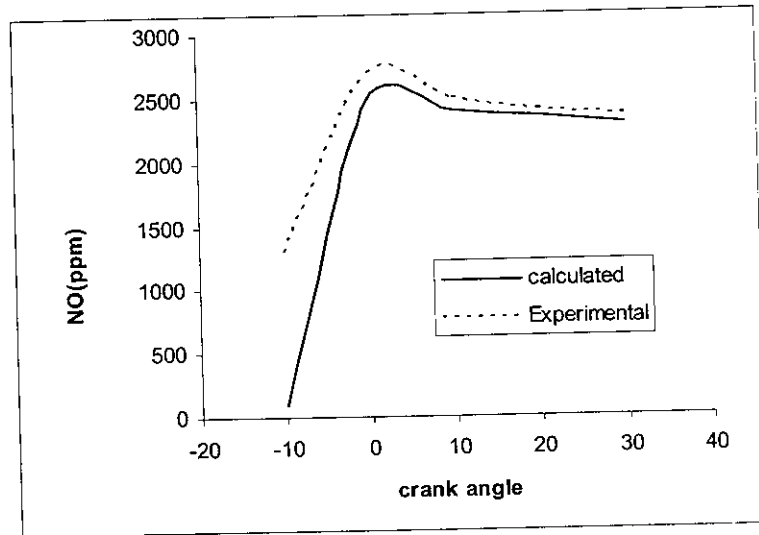


FIG 3.5 COMPARISON OF CALCULATED AND EXPERIMENTAL NITRIC OXIDE

The problem of NO production in naturally aspirated (NA) diesel engines arises from the early rapid burning, which produces very-high-temperature products. Recall from previous discussions that if the reactants have stoichiometric or slightly lean fuel-air ratio the amount of NO produced will be maximum. In NA engines with MBT injection timing, evidence from sampling and radiation measurements indicate the reactants are lean or stoichiometric during the premixed burning.

Figure 3.5 shows a comparison of the NO history in the cylinder calculated from calculated and experiment for heavy duty engine with direct injection. The problem of NO production in modern heavy-duty turbocharged diesels with high-pressure injection and restarted timing is more complex. Again, by use of total cylinder sampling, data show that in such engines a significant portion (40%) of the NO_x is produced after peak pressure, and that the premixed burning could at most produce less than half of the NO_x produced at peak pressure. However CFD calculations using only Zeldovich kinetics have been able to reproduce the experimental NO histories remarkably well. These models NO values are, however, very sensitive to the ignition and turbulence models so that the excellent agreement may be caused by fortuitous combinations of these sub models.

Two methods of reducing NO emissions are quite effective. The first method is to retard the injection timing. This causes some reduction in fuel economy, but is quite effective because it reduces the amount of premixed burning. The second method is to recirculate cooled exhaust gas so that product temperatures are lowered. These solutions when combined solve the NO problem, but unfortunately both methods increase the amount of exhaust particulate.

At the present time no proven method of simultaneously reducing NO and particulates is known. We do know that a great portion of the [particulate produced is oxidized in the cylinder. Only 1/10 to 1/20 of the soot formed escapes into the exhaust. The largest peak in soot production is just at the start of diffusion during when the fuel spray is cut off from its air supply and surrounded by very hot products from the premixed burning. However, the high temperature and subsequent mixing with air cause this soot to rapidly oxidize. Furthermore, the time for the soot particles to agglomerate at this time is very short. Soot produced later, near the end of burning, is less likely to be oxidized because the temperature is much lower due to expansion. Soot remaining from the previous combustion is now also slower to oxidize, because of the lower temperature.

Modeling of the soot production-oxidation process is hampered by the present inability to predict soot production and to a lesser extent by the uncertainty of agglomeration, oxidation and mixing models. It is clear, however, that neither very rapid mixing nor very slow mixing models. It is clear, however, that neither very rapid and thus quench oxidation. Slow mixing will prevent oxidation due to the low partial pressure of oxygen, and cooling by expansion will eventually prevent further oxidation. The optimum path of fuel/air ratio during combustion and rate of mixing of products with air is unknown. We can see, however, that both retarded injection and exhaust gas recirculation produce more soot due to more diffusion burning, less oxygen, and lower oxidation temperatures.

P-1690

Chapter 4

Turbulent flow and model

4.1 TURBULENT FLOW

Turbulent Flow is important in engineering applications because it is evolved in the vast majority of fluid flow and heat transfer problems encountered in practice. The term turbulent is used to denote that the motion of the fluid is chaotic in nature and involves crosswise mixing or eddying superimposed on the motion of the main stream. According to Von Karman and Taylor "Turbulence is an irregular motion which in general makes its appearance in fluids, gaseous or liquid, when they flow past solid surfaces or even when neighboring streams of the same fluid flow past or over one another". The flow pattern in turbulent flow is so complex that they cannot be completely predicted mathematically even for simple passage geometries.

If a chunk of fluid is bodily moved in an irregular manner, then, with respect to a stationary observer, the motion is irregular in time. The fluid viscosity will cause the conversion of some of the kinetic energy of the flow into heat. Thus turbulent flow, like all flow of viscous fluids, is dissipative in nature. If there is no external source of energy for the continuous generation of turbulence, the turbulent or irregular motion with a flow will decay. It is believed that the fluctuations inherently come from disturbances and they may be either damped out due to viscous damping or may grow by drawing energy from the free stream.

The Reynolds number, Re of a flow gives a measure of the relative importance of inertia forces and viscous forces. If Re is below a critical value the flow is smooth and adjacent layers of the fluid slide past each other in an ordinary fashion. If the applied boundary conditions do not change with time the flow is steady and the regime is called laminar flow. In laminar flow condition, the kinetic energy from the mean flow is not enough to sustain the random fluctuation in the face of viscous damping and in such cases laminar flow continues to exist. At Reynolds number higher than the critical value, the energy drawn from the mean flow supports the growth of fluctuations and transition to turbulence is induced. The velocity and all other properties such as pressure, temperature and species concentration vary in random manner with time, even with steady boundary conditions. This regime is called turbulent flow.

4.2 CHARACTERISTICS OF TURBULENT FLOW

1. 'No slip' conditions is satisfied at the boundary
2. Turbulence is generated due to instability of flow in regions of higher shear, i.e., near boundary or at the interface of two moving layer. The former is called 'wall turbulence' while the later is called 'free turbulence'
3. In turbulent flow, however because of chaotic cross wise eddying of fluid particles between the stream lines, the properties such as velocity, pressure, temperature, etc, at any point vary continuously with respect to time.
4. Therefore in the analysis of turbulent flow the instantaneous Values of the properties are represents as a sum of a time - Averaged mean part and a fluctuating part in the form.

$$U_i = u + U'$$

$$V_i = v + V'$$

$$T_i = T + T'$$

$$P_i = P + P'$$

Where, U_i, V_i, T_i, P_i are the instantaneous values; U, V, T, P the time averaged values; and U', V, T', P' are the functions.

5. Vigorousness of turbulence at a given point is measured by turbulence intensity.
6. Turbulent flow is a characterized by the presence of circulatory a fluid mass known as eddies. At any time, the eddies of a wide Spectrums of sizes are present in the flow.
7. The largest eddy will be of the size of the flow it, self, e.g. pipe diameter or depth of flow in a channel. The smallest eddy will be extremely small.
8. Presence of eddies in the flow makes it capable of efficient transport of momentum, mass or energy across the flow.
9. Large eddies capture energy form the mean flow; they break into smaller and smaller eddies until eddy Reynolds number, (size of eddy X characteristic Turbulence velocity / kinematics Viscosity), become very small.
10. Ultimately the small eddies s die out and their energy is dissipated

energy loss than in laminar flow. Head loss is proportional to the square of mean velocity.

11. Turbulent flows are highly diffusive (rapid mixing). Diffusion rates in turbulent flow can be 10 to 100 times molecular diffusion rates.
12. Turbulent flows are highly dissipative (energy is converted into heat due to viscous stress).
13. 3- Dimensional (even if the mean flow is only 2D)
14. Turbulent flows are the major source of energy loss.
15. Turbulence needs a mean velocity gradient to sustain itself.
16. To viscosity and shear stress due to turbulence. Loss of pressure loss is approximately proportional to the square of velocity.
17. Presence of turbulent fluctuations in velocities causes additional normal and tangential stress.
18. For turbulent flow the total shear is the sum of shear stress due to viscous and due to turbulent stress.
19. Turbulent flows have vortices.
20. Turbulent flow has well defined spatial structures.

4.3 CONCEPT OF EDDY

In turbulent boundary layer flows, momentum is continuously transferred from the boundary towards the outer flow. Part of this transfer mechanism is such that low momentum fluid at the wall is periodically gathered into blobs which are then pulled upwards into the faster outer current. These blobs are called turbulent eddies. Turbulent eddies are not rigid bodies like molecules and do not retain their identity. There is a range of eddy sizes; the largest size is determined by the characteristic dimension of the flow and the smallest size is determined by fluid viscosity. Small eddies join and become big eddies breakup into smaller eddies. The large eddies are responsible for extracting the energy from the mean motion and feeding it into the turbulent motion.

4.4 CLASSIFICATION OF TURBULENT FLOW

Turbulence can be generated by frictional forces at confining solid walls or by the flow of layers of fluids with different velocities over one another. Turbulence generated in these two ways is distinctly different. According to generation turbulence is classified as

1. Wall turbulence
2. Free turbulence
3. Free stream turbulence

Turbulence generated and continuously affected by fixed walls is known as wall turbulence and generated by two adjacent layers of fluid in absence of wall is termed as free turbulence. Turbulence produced externally but transported within the system being studied is called free stream turbulence. Turbulence is called isotropic. If its statistical features have no directional preferences and perfect disorder persists. Isotropy is seen in applications where the gradient of the mean velocity is zero, i.e. the mean velocity is either zero or constant. When the mean velocity has a gradient, turbulence even if initially isotropic will grow to become anisotropic. The term turbulent shear flow is often used to refer to this kind of flow, near-wall flows, boundary layers, mixing layers and jets fall in this category.

4.5 TURBULENCE MODELING

The basis of turbulence modeling is to decompose the instantaneous velocity of the fluid into a mean and a fluctuating component, and solving for the mean velocity, while the effect of the fluctuating components on the mean motion is modeled after empirical relations obtained for specific cases from experiments. The Navier – Stokes equations together with the equations of mass conservation form a closed system of equations. When the velocity components are decomposed we have more unknowns than the number of available equations. The modeled system of equations cannot be closed within itself unless empirical relations are supplied from experiments to correlate the fluctuating components with mean motion. This is termed as the closure problem.

Turbulent flows exhibit a largely enhanced diffusivity. The turbulent diffusion greatly enhances the transfer of mass, momentum, and energy. The apparent stresses, therefore, may be of several orders of magnitude greater than in the corresponding laminar case.

4.6 REYNOLDS TIME AVERAGING

A Turbulence model is defined as a set of equations (algebraic or differential) which determine the turbulent transport terms in the mean flow equations and thus close the systems of equations.

Turbulence models are based on hypotheses about the turbulent processes and require empirical input in the form of model constants or functions. They do not simulate the details of the turbulent motion, but only the effect of Turbulence on the mean flow behaviour. The concept of Reynolds averaging and the averaged conservation equations are some of the main concepts that form the basis of Turbulence modeling.

Since all turbulent flows are transient and three dimensional, developing methods for averaged quantities gives useful information. The most popular method for dealing with turbulent flows is Reynolds averaging which provides information about the overall mean flow properties

The main idea behind Reynolds time – averaging is to express any variable ($\phi(x,t)$) which is a function of time and space, as the sum of a mean and a fluctuating component as given by

$$\phi(x,t) = \overline{\phi(x,t)} + \phi'(x,t) \quad (4.1)$$

Here the notation of upper dash denotes the time average of the flow parameter. For stationary turbulence, this average is defined by

$$\overline{\phi(x)} = \overline{\phi(x,t)} = \lim_{\tau \rightarrow \infty} \frac{1}{\tau} \int_t^{t+\tau} \phi(x,t) dt \quad (4.2)$$

By definition, the average of the fluctuating components is zero. Here we use the notation that the upper case symbols denote the time average of that quantity. For engineering applications it is assumed that it is much greater than the time scale of the turbulent fluctuations.

4.7 TURBULENCE PARAMETERS

The initial inlet flow of the IC Engine is not known completely, but it was assumed that there pre exists a specific amount of Turbulence in the flow field. The computational algorithm uses parameters that are related to the creation and dissipation of turbulence, some like the intensity and length scale parameters, are based on the assumption that the characteristic velocity and the characteristic length of the larger turbulent eddies in the solution are of the same order as the velocity and length scale of the mean flow, a major assumption of CFD turbulence models. IC engine flows vary in the turbulence characteristics, with turbulence intensity factors being as low as 0.05 %.

The choice of these turbulence parameters are used for the inlet BC's and will change as the model solves. The converged solution should be independent of the initial values, yet it is important to start with reasonable values for the k and e , as it affects the downstream flow. Other turbulence factors can be derived from these numbers, including the modified Turbulent viscosity and the specific Dissipation rate another, separate, parameter used to define the Turbulence in CFD models in the Turbulent Viscosity ratio. This ratio is directly proportional to the turbulent Reynolds number, which is defined in terms of the turbulent kinetic energy, the dissipation rate and the viscosity, and is usually in the range of a value between one and ten.

Mean velocity

Mean velocity is defined as an ensemble average velocity obtained from instantaneous velocity obtained from instantaneous velocity profiles around which the fluctuations of velocity take place. It varies with time or crank angle in engine flows. Its magnitude is evaluated from the equation given below.

$$\bar{U}(\theta) = \frac{\sum_{i=1}^N U(\theta, i)}{N} \quad (4.3)$$

Turbulent intensity:

Turbulent intensities are given by the quantities. Where the fluctuating part of the turbulent velocity component and is the mean velocity component.

Turbulent intensity is refers to as the root mean square value of the fluctuating component of velocity and is an indication of the strength of eddy internal recalculation . The parameter is most commonly used by the researchers to relate the flow field to the turbulent combustion process. This is also calculated by ensemble averaging procedure indicates as

$$U'(\theta) = \left[\frac{\sum U(U(\theta, i) - \bar{U}(\theta))^2}{N} \right]^{1/2} \quad (4.4)$$

Relative Turbulence Intensity:

Relative turbulence intensity (RTI), indicated below, is a measure of turbulence intensity in relation with mean velocity and is an indicator of the flow field activity.

$$RTI = \frac{U'(\theta)}{\bar{U}(\theta)} \quad (4.5)$$

Turbulent kinetic energy

The turbulent energy included by this flow, on assumption that is released to the kinetic energy created. The incremental kinetic energy value at each time step is dKE_{sq} , where

$$dKE = \frac{dm_{sq} c^2_{sq}}{2} \quad (4.6)$$

4.8 TURBULENCE MODEL EQUATIONS

4.8.1. Turbulence Model

Various models were utilized to study the rotating cylinder in the wind tunnel and varied considerably in the results. The total number of choices and sub-choices are staggering. Excluding the variations of the setting of initial conditions, which varied from model, as well as excluding energy solution parameters, the total number of turbulent model options exceeds 50, if one includes the choices of wall treatments for each model. Without direct experience with each specific model, it is difficult to choose the best one for our scenario. For example, it is difficult to know on what scale “swirl” is fluid dynamically defined without seeing computational examples of it. Many models were tried, and many failed. The basis of each turbulence model is discussed here.

4.8.2 Spalart-Allmaras Turbulence Models

The Spalart – Allmaras is a one equation (in addition to the general transport equations) Turbulence model which solves for the turbulent eddy viscosity, and eliminates the need to calculate the length scale related to local turbulence. Although designed to be used with meshes that fully resolve the inner Boundary layer (i.e. cells with y^+ values of 1-11.25), in which case the enhanced wall treatment option should be selected, it has been shown to be adequate for coarser meshes if the wall function option is chosen. When using this model, the strain / vortices separation, as it includes the effects of the mean strain due to rotational velocity gradients. My runs show mixed results with the Spalart Allmaras.

4.8.3 K-e Turbulence Models

The K-e models are the workhorse of the CFD industry, and have been shown to be robust in a variety of applications. K-e models use two equations to calculate turbulent Reynolds stresses, based on calculations of turbulent kinetic energy (k), and turbulent dissipation (ϵ). The K-e model uses additional constants based on empirical data from a wide range of flows. However, although the

bit of fudge, as there are many unknown and immeasurable terms in the dissipation equations. The basic assumption is that turbulent dissipation is on the same order of the turbulent production term, and the K-e model applies mostly to flows that are fully turbulent. Where the effects of molecular viscosity are negligible. The model has problems with flows that have curved boundary layers, as our rotating cylinder problem does; yet it was used for many of the runs in the results because of its consistent results. Besides the standard K-e model, two more variations are available in fluent.

The RNG model also uses two equations for turbulence kinetic energy and dissipation, yet has different constants and calculates the effective viscosity differently. It is considered more responsive to flows with high stream line curvature. Two options are available with RNG: "differential viscosity" which accounts for low Reynolds number changes to turbulent viscosity calculations and used for flows, which have significant swirl. When using the RNG model, it is recommended to begin with a solved solution from the standard K-e model, although I didn't have much luck with this technique. The third k-e model is the realizable model. This uses a similar equation for turbulent kinetic energy, but calculates turbulent dissipation independent of the rate of production. This makes the model more likely to diverge with a poor model, but is shown to produce better results for flows which include missing layers and boundary separation. Good results were had with the Realizable model.

4.8.4 K-omega Turbulence Model

The K-omega model also uses two equations to represent the turbulence, but instead of ϵ , it calculates a specific turbulence dissipation rate, which can be considered the ratio of ϵ to k . It is recommended for low Reynolds number flows and does not offer the standard wall function choices in fluent, as by default, it uses the enhanced wall treatment when the mesh is fine enough, and uses wall functions when the mesh elements are not placed entirely within the boundary layer. The SST (Shear - stress Transport) K - omega model takes in to account the transport of turbulent shear stress... and makes a gradual change of solution

layer to a high Reynolds number version of the K- ϵ model in the outer part of the boundary layer. The SST K- ω model is more reliable for flows that have adverse pressure gradients, and would be the proffered model, of the two K- ω choices for the K- ω model include transitional flows (a low Reynolds number correction to turbulent viscosity), and for the standard K- ω model, shear flow corrections.

4.8.5 Reynolds's Stress Equation Turbulence models

The most advanced (requiring the most computational resources) classic turbulence model is the Reynolds's Stress Model (RSM), which use equations to solve directly for the Reynolds stresses. Five additional equations are involved the 2D model (seven 3D) and because it makes fewer assumption about the turbulent eddy formations and dissipations. It is considered the "simplest" and most accurate of the turbulence models for fluid flows.

4.8.6 Recommendations

The standard K- ϵ model with enhanced wall functions is the model that seemed to work overall the best for my models, despite its not being recommended for problems due to the high pressure gradients and separated flow. There were also good runs with the k- ϵ Realizable with enhanced wall functions. Other possible models would include the K- ω SST with the transitional flows option, and perhaps even the spalart Allmaras with the strain/vorticity and with standard wall functions, for the coarser meshes

Chapter 5

*Computational fluid
dynamics*

5.1 INTRODUCTION

Fluid flow is governed by the conservation of three fundamental quantities namely mass, momentum and energy. The description of these conservation laws in mathematical form yields non-linear partial differential equation, which is famously known as the Navier-stroke equation. Although these Navier-stroke equations have been known since the 1800s, they have been too difficult to solve for arbitrary flows until the development of the modern computer. The science involved in solving these equations numerically on the computer is known as computational fluid dynamics (CFD)

In order to solve the Navier-Stokes equations, the flow domain for the specific problem is first discretised. Domain discretisation, using mesh or grid generating techniques, involves breaking up the selected control volume into smaller volumes and solving the Navier-Stokes equations over each volume. For simple geometries such as rectangular shapes, discretisation is simple but gets more difficult as the geometry becomes more complex. Also, to accurately capture flow phenomena such as turbulence, fine grids are required at the region of interest leading to an increased number of mesh elements. This results in a large system of non-linear equations requiring large computing memory. However, with the ever-increased computing capability available today, a lot of complex flow problems can now be solved.

Commercial CFD codes such as FLUENT, PHOENIX, CFX, CFD++ and Star-CD have also developed to a point that the user need not be an expert on CFD in order to successfully put it to use. The end-user must however have a good knowledge of fluid dynamics for a successful simulation with credible results to be obtained. Therefore, used correctly, CFD codes can reduce time and cost of experiments in product development or process improvement.

The rest of the chapter discusses the various areas of CFD in the following order:

- Governing equations
- Grid generation techniques
- Boundary conditions that define a CFD problem
- Solution algorithms and convergence criteria
- Basic background on the CFD solver used (FLUENT)

5.2 GOVERNING EQUATIONS

The governing equations of fluid behavior are given in equations. These equations are given for compressible flow, but can be easily simplified for incompressible flow. In the Eulerian system, the particle derivative is described as follows

$$\frac{D}{Dt} = \frac{\partial}{\partial t} + (\bar{V} \cdot \nabla) \quad (5.1)$$

Where:

$$(\bar{V} \cdot \nabla) = d\bar{V} = \frac{\partial u}{\partial x} + \frac{\partial V}{\partial y} + \frac{\partial w}{\partial Z} \quad (5.2)$$

This particle derivative will be used in the sections to follow to present the Navier-Stokes equations in conservative form.

5.3 CONSERVATION OF MASS

The equation for conservation of mass in conservative form is given as:

$$\frac{\partial \rho}{\partial t} + \nabla \cdot (\rho \bar{V}) \quad (5.3)$$

Where ρ is the density and \bar{V} is the vector velocity of the fluid.

5.4 CONSERVATION OF MOMENTUM

The equations for conservation of momentum in the three Cartesian directions can be rewritten as a single vector equation using indicial notation:

$$D\rho\bar{V} = \rho\bar{a} = \rho \frac{\partial}{\partial t} \left[u \left(\frac{\partial v_i}{\partial x_j} + \frac{\partial v_j}{\partial x_i} \right) + \delta_{ij} \rho \bar{V} \right] \quad (5.4)$$

5.5 ENERGY EQUATION

The energy equation, which in essence is the first law of thermodynamics, is given in its most economic form as follows:

$$\rho \frac{D}{Dt} \left[e + \frac{p}{\rho} \right] - \frac{Dp}{Dt} + d(KVT) + \tau_{ij} \frac{\partial u_i}{\partial x_j} \quad (5.5)$$

Where the viscous stresses are given by the stress tensor:

$$\tau_{ij} = \mu \left(\frac{\partial u_i}{\partial x_j} + \frac{\partial u_j}{\partial x_i} \right) \quad (5.6)$$

5.6 FLOW STRUCTURE

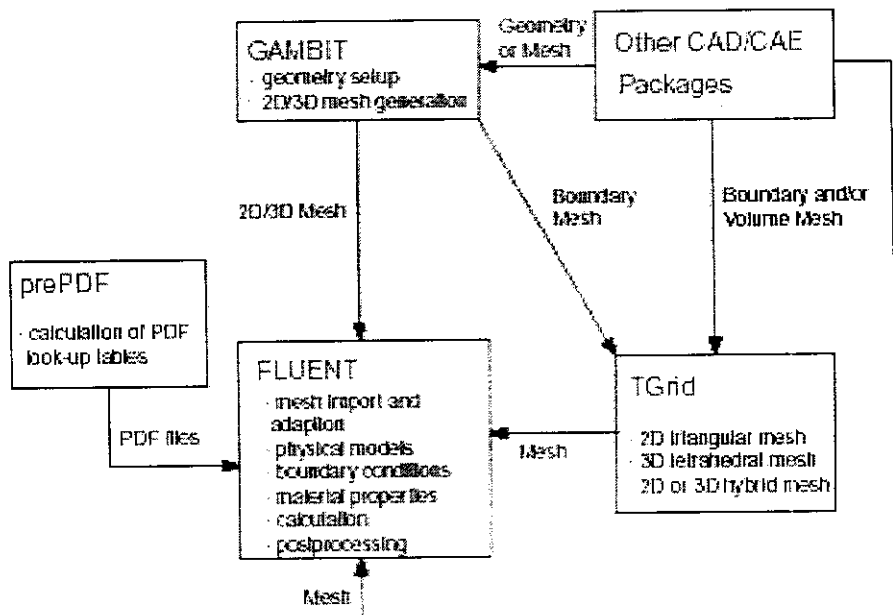


FIGURE 5.1 BASIC FLOW STRUCTURE

The figure 5.1 shows the flow structure of FLUENT package includes the following products:

FLUENT - the solver.

PrePDF - the preprocessor for modeling non-premixed combustion in

- GAMBIT - the preprocessor for geometry modeling and mesh generation.
- Tgrid - an additional preprocessor that can generate volume meshes from existing Boundary meshes.
- Translators - (translators) for import of surface and volume meshes from CAD/CAE packages such as ANSYS, CGNS, I-DEAS, NASTRAN, PATRAN, and others.

You can create your geometry and grid using GAMBIT. See the GAMBIT documentation for details. You can also use Tgrid to generate a triangular, tetrahedral, or hybrid volume Mesh from an existing boundary mesh (created by GAMBIT or a third-party CAD/CAE Package). See the Tgrid User's Guide for details. It is also possible to create grids for FLUENT using ANSYS (Swanson Analysis Systems, Inc.), CGNS (CFD general notation System), or I-DEAS (SDRC); or MSC/ARIES, MSC/PATRAN, or MSC/NASTRAN (all from MacNeal-Schwendler Corporation). Interfaces to other CAD/CAE packages may be made Available in the future, based on customer requirements, but most CAD/CAE packages can export grids in one of the above formats.

Once a grid has been read into FLUENT, all remaining operations are performed within the solver. These include setting boundary conditions, defining fluid properties, executing the solution, refining the grid, and viewing and post processing the results. Note that preBFC and GeoMesh are the names of fluent preprocessors that were used before the introduction of GAMBIT. You may see some references to preBFC and GeoMesh in this manual, for those users who are still using grids created by these programs.

5.7 Grid generation and GAMBIT

The grid generation process or meshing involves dividing the flow domain into smaller control volumes over which the discretised Navier-Stokes equations are solved. Grid (mesh) types can be classified into two categories namely; structured and unstructured grids. The mentioned types of grids find use in

Structured grids consist of grid lines with a characteristic of not crossing or overlapping. The position of any grid point is uniquely identified by a set of two (2-D) or three (3-D) dimensional indices, e.g., (i, j, k) . Unstructured grids make no assumption about any structure in the grid definition and usually consist of triangular (tetrahedral (ted) in 3D) elements.

A numerically generated structured grid or mesh is understood here to be the organized set of points formed by the intersections of the lines of a boundary conforming to a curvilinear coordinate system. The prime feature of such a system is that some coordinate line (surface in 3D) is coincident with each segment of the boundary of the physical region.

The use of coordinate line intersections to define the grid points provides an organizational structure that allows all computations to be done on a fixed square grid when partial differential equations of interest have been transformed so that the curvilinear coordinates replace the Cartesian coordinates as the independent variables. This grid frees the computational simulation from restriction to certain boundary shapes and allows general flow solvers to be written in which the boundary shape is specified simply by input.

Grid generation for the purposes of this research takes place in FLUENT's pre-processor, GAMBIT. GAMBIT is a versatile pre-processor that can support a large variety of commercially available computer-aided design (CAD) platforms. Raw geometry can be imported from these CAD packages into GAMBIT where it is operated on (i.e., the necessary simplification for CFD purposes are made), in preparation for meshing.

Various meshing schemes are available in GAMBIT and are used where suitable in the grid generation process. Most of these schemes are unique to GAMBIT and are not necessarily documented, as they may be modifications of existing meshing schemes. GAMBIT allows the user to specify any volume to be meshed, although the shape and topological characteristics of the volume determine which mesh schemes can be used.

Different meshing schemes such as Hex, Hex/wedge and Tet Hybrid, can

elements only constituting a fully structured mesh. The Hex/wedge mesh comprises mainly of hexahedral elements with wedge elements where necessary. However, Hex and Hex/wedge elements do not apply to any shape volume, as opposed to Tet Hybrid meshes. The versatility of the Tet Hybrid element makes it appreciable for use where the volume is complex and none of the other meshes can be applied. Solution inaccuracies associated with the Tet Hybrid element type are, however, more significant than for any of the other element types. Each element type is associated with a volume-meshing scheme and only those schemes used in this study will be discussed.

Cooper meshing scheme

When this scheme is enforced on a volume, GAMBIT treats the volume like a cylinder with end-caps. In the actual volume, the faces at these locations are representative of the end-caps and are called source faces. They are so-called because their face meshes are projected through the volume after certain mesh operations have been performed by GAMBIT as is illustrated by Figure.

The Cooper scheme involves, in order of occurrence, the following steps:

1. Meshing the non-source faces
2. Imprinting the source faces on one another
3. Meshing the source faces
4. Projecting the source faces' node patterns through the volume to produce a volume mesh.

The steps described can be illustrated by the example in Figure 5.2, which shows the union of a prism, cylinder and a rectangle.

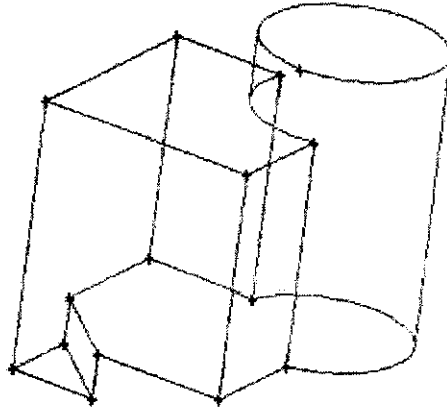


FIG 5.2 UNION OF CUBE, A CYLINDER, AND A TRIANGULAR PRISM

The various Cooper mesh scheme steps are clearly illustrated in Figure 5.3.

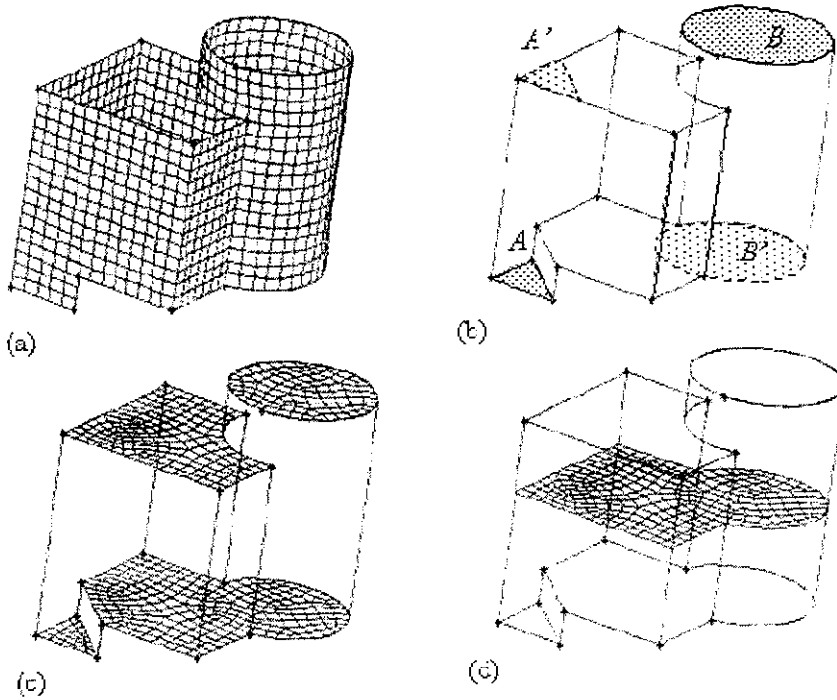


FIG 5.3 COOPER MESHING SCHEME

5.8 Boundary Conditions

Equations presented in the preceding section remain the same regardless of the flow field, i.e., external flow, internal flow, two-phase flow (with some modifications), etc. In mathematics, any solution to a set of partial differential equations (PDE's) requires a set of boundary conditions for closure and the solution of the governing equations is no exception.

CFD simulations largely depend on the boundary conditions specified; hence correct boundary specification improves convergence to a correct solution. Incorrect boundary and initial conditions, however, can give convergence although not to a correct solution.

There is a wide variety of boundary types available in FLUENT, but only those used in this study will be given.

1. Flow inlet and exit boundaries

Pressure inlet: Used to define the total pressure and other scalar quantities at flow inlets.

Pressure outlet: Used to define the static pressure at flow outlets (and also other scalar variables, in case of backflow). The use of a pressure outlet boundary condition instead of an outflow condition often results in a better rate of convergence when backflow occurs during iteration. Note that when backflow occurs, this boundary acts like a pressure inlet boundary.

2. Wall and symmetry:

Wall: Used to define a solid-fluid interface where viscous flow is considered, thus applying a no-slip condition. The boundary condition on a surface assumes no relative velocity between the surface and the gas immediately at the surface.

Symmetry: Used to define surfaces at which normal velocity and normal gradients of all other variables are zero. This boundary type is essential where the geometry is symmetrical in nature.

5.9 SOLUTION ALGORITHMS

The governing equations of fluid flow are particularly difficult to solve because of their non-linear nature. Much work has been done in numerical methods to solve for these types of equations. Some proven and popular methods worthy of note are SIMPLE, SIMPLE-C, SIMPLER, QUICK and PISO. These methods are appreciated because of their robustness when applied to a variety of problems. In this study, steady-state and transient flows are solved using the SIMPLE and PISO algorithms respectively.

The acronym, SIMPLE, stands for Semi-Implicit Method of Pressure-Linked Equations, and describes the iterative procedure by which a solution to discretised equations is obtained. This method is well suited to steady-state solution computation. The iterative procedure is the pseudo-transient treatment of the unsteady governing equations in a discrete form to obtain a steady-state solution.

PISO, which stands for Pressure-Implicit with Splitting of Operators, is a pressure-velocity coupling scheme that is part of the SIMPLE family of algorithms. This scheme is based on the higher degree of the approximate relation between the corrections for pressure and velocity. In highly distorted meshes, the approximate relationship between the correction of mass flux at the cell face and the difference of the pressure corrections at the adjacent cells is very rough. An iterative process is required to solve for the pressure-correction gradient components along cell faces since they are not known beforehand leading to the introduction of a process named skewness correction. Here, the pressure-correction gradient is recalculated and used to update the mass flux corrections after the initial solution of the pressure-correction equation is obtained. This process significantly reduces convergence difficulties associated with highly distorted meshes and allows FLUENT to obtain solution on a highly skewed mesh in approximately the same number of iterations as required for a more orthogonal mesh.

5.10 CONVERGENCE

Convergence of a flow or heat problem can be judged by observing the normalized residuals. Residuals are numerical imbalances from the solved governing equations resulting from an incomplete solution during the iterative process. The solution process can be terminated when the normalized residuals fall below a specified value, which is generally 10^{-3} . However, in some cases even with the convergence criteria (as far as normalized residuals are concerned) satisfied, the solution may not necessarily be a correct one. To avoid such instances, quantities such as mass flow rate, static pressure and heat flux can be monitored at a location in the flow domain that is deemed to be important. The monitored quantity is observed until the change from iteration to iteration is negligible thus ensuring good convergence.

5.11 BACKGROUND ON THE CFD SOLVER

FLUENT is a finite volume (FV) solver that can handle a wide variety of flow problems such as external flow, internal flow, and two-phase flow. All modes of heat transfer can also be solved by the CFD code. This code is used for all CFD analyses throughout this study.

Modern CFD packages are user-friendly with improved user and code interfacing. Thus understanding the underlying principles of flow is important in order to put the code to good use. FLUENT has a facility for coding to make repetitive simulations, as in an optimization loop, more efficient and hence save time. This facility makes use of a journal file, which is a file containing a list of text commands that set-up a CFD model and runs the simulation. Post processing can also be performed with the use of these journal files. Thus, the code is very suitable for a wide-variety of industrial problems including the one that is the subject of this study.

5.12 CFD MODELING OF DIESEL ENGINE

The intent in the following review of the status of CFD models for diesel combustion is to motivate the reader to further study and to indicate how such

models must be

combined with past experience and experiments to be effective. The models for diesels form a hierarchy consisting of simple analysis models, zero-dimensional models, quasi-one dimensional models, phenomenological models, and CFD models. The engineer must learn to use all of these tools both experimental; and theoretical, in concert. There is no perfect model and each must be used within the scope of its ability to predict. Sometimes the models can be used only to motivate experiments, sometimes to improve understanding or predict trends, and sometimes to make quantities predictions that can be used directly in design. However in no case do they yet substitute for good judgment experience.

5.12.1 Grids and grid - element equations

Because internal combustion engine valves and combustion chambers represent a complex geometry, the grid generation problem is complex and must conform to moving boundaries created by the moving piston and valves. In addition, some regions such as the port near the valve and around the injector tip region require fine grids to resolve the flow, because engine boundary layers. Given these important issues it is no wonder that grid generation and numerical techniques for reconstructing grids efficiently are the subject of a large block of literature. As CFD programs begin to be used in application, the importance of quick and inexpensive grid generation is bound to increase.

A typical means of reducing both the grids generation and computational effort is to assume zonal symmetry at the time of injection and there after. Thus, for a nozzle located coaxially with the cylinder and having equally spaced holes, one calculates for a Pie - shaped zone of included angle $360^\circ/n$. The figure 5.4 shows a typical grid for cylinder of a DI engine. The grids for valves are used to generate intake flows. Because the flow field prior to injection is not symmetric, the zonal symmetry models represent a compromise between accuracy and cost.

The conservation equations of mass, momentum, and energy include turbulent diffusion terms. The mass conservation equation for a given species includes terms for sources due to Fick's law, chemical reactions, and spray

includes the turbulent kinetic energy , the turbulent viscous stress tensor , and the momentum gain due to the spray. The energy equation uses source terms to include chemical heat release. Spray interactions, turbulent s heat conditions, and turbulent enthalpy diffusion. The turbulence is modeled by the $k-\varepsilon$ model, but now must include source terms for interactions with the spray. Again, the turbulent diffusion co-efficient is taken proportional to k^2 / E .

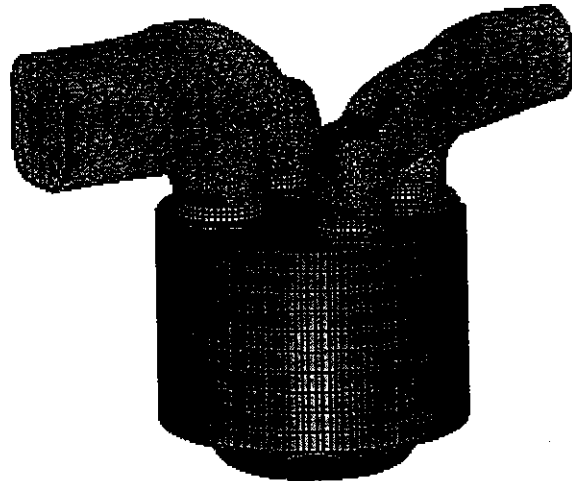


FIG 5.4 COMPUTATIONAL MESH FOR CFD SIMULATION OF ENGINE

5.12.2 Spray model

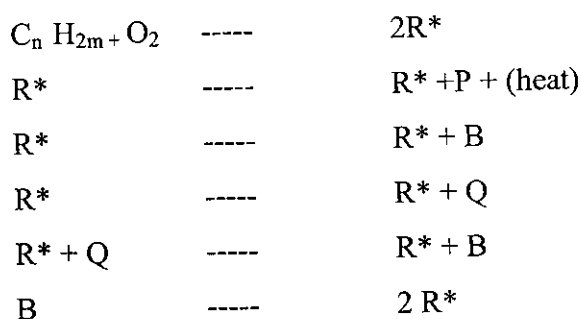
For diesels are fully warmed up conditions, the droplets, which are very small (10 μ m), vaporize rapidly. However, for starting or for small engines the liquid spray impinges on the piston. This can lead to instantaneous break up as droplets rebound, vaporization of a thin liquid film on the surface, and sliding or bouncing back of droplets with dissipation of their shape. The gas entrained by the moving droplets also enhances the convective effects on vaporization and heat transfer at the surface. The effects of surface deposits on these phenomena are not quantified, but it is known that liquid fuel can be trapped in the deposits, delaying its release as vapor.

For cold starting the effects of fuel volatility are important , and thus modeling of how various species vaporize from real fuels. One may, for example ask how a volatile fuel fraction of high cetane number aids ignition. Multicomponent droplet vaporization models seem to be required and such

improvements are now being introduced. However diesel cold starting is quite ill behaved. For example, a cylinder may fire, then not fire again for a cycle or two before firing again. This suggests some mechanisms of fuel is stored in surface deposits or crevices. Thus droplet model may not be sufficient to explain starting behaviour.

5.12.3 Ignition model

Because low – temperature chemical kinetics plays a role in diesel ignition, the process should be modeled by mechanisms including effects of branching reactions and possibly two stage ignition. To keep such calculations within the bounds set by current computing capacity, reduced mechanisms have been favored for use in CFD codes. The model used for diesel CFD ignition by the bold and cheng and more recently by Kong and reitz is the so – called “Shell Model”. This model has eight generic equations with eight rate constants. The equations for ignition of $C_n H_{2m}$ fuel in air use a generic radical pool (R^*), an intermediate species(Q), and a branching agent(B) to produce CO , CO_2 and H_2O products (P)



In order to use this model for a given fuel, one must if rate constants to combustion bomb data. Because the equations are not elementary, differences between bomb and engine conditions may influence the results. In particular, the sensitivity to local temperature means that the CFD code must be validated in conjunction with the ignition model. Errors in prediction should thus not all be attributed to the ignition model. The results of Kong and Reitz [1993] show quite good agreement with engine data, but the range of data and fuels is still too limited to judge the success. It may be that the model will always require some

given fuel shows excellent validation over a range of initial pressures and temperatures. When split injection is used, the second injection into higher-temperature gases which may contain radicals. Visualization diagnostics show that the ignition can take place instantly as soon as the fuel leaves the nozzle.

5.12.4 Combustion

A characteristic time model based on earlier eddy breakup models has been tuned for diesel conditions. Recall that the characteristic time scale consists of a "laminar time scale" and a "turbulent time scale" modified by a factor f^* . The value r depends on the ratio of products to total reactive species and thus goes from 0 (no reaction) to 1 (complete consumption of fuel). Thus, for diesel combustion the rate of premixed combustion is under conditions where r is nearly zero; that is, the local value of $f = (1 - e^{-r}) / 0.632 = 0$. Thus the time constant depends mostly on the laminar time constant during the premixed period. In spark ignition engines this initial period is the kernel growth period, but in diesels it appears that the early combustion is dominated by chemical kinetics, not flame propagations.

The laminar time constant is thus derived from chemical rate expressions. Once combustion starts, the pressure rises rapidly and many cells of mixture may become autoignition. To take care of this, the shell model is not used for cells with $T > 1000$ K and is replaced by the combustion model rate obtained from this CFD model and a single-zone analysis based on experimental pressure history is used in the single-zone model, the HRR agrees with KIVA prediction. The ignition delay and premixed spike show excellent agreement, but the transition from premixed to mixing control is not as well modeled, resulting in a small error in peak pressure. The combustion model paid only one part in the HRR; the spray and mixing models play important roles too. Thus it is difficult to judge which model needs improvement or if any of the models are correct, because they have all been adjusted based on overall engine measurements.

5.12.5 Emissions models

The primary diesel exhaust emissions of NO_2 and particulates are both very

P-169

model NO_x well and provided that the HRR and mixing are properly modeled. First attempts to model NO_x using the $K-\varepsilon$ turbulence model and also reproduced the total cylinder NO_x histories obtained by dumping experiments. Many issues can play a part in such computations. But it is doubtful that the kinetic mechanism itself is a major source of error. Temperature seemed to be a major source of error, because the standard $K-\varepsilon$ model called the RNG $K-\varepsilon$ model produced a smaller turbulent viscosity and higher temperatures resulted. Note that the engine modeled has a smaller than conventional spray angle, so that the spray impinges on the bowl bottom rather than on the bowl vertical side as is more typical. The higher temperatures of the modified model caused the correction factor to go from 62 to 0.78. It compares the shapes of NO_2 curves for the two turbulence models, each corrected by a constant factor to make them agree with the experimental value as measured in the exhaust.

The fact that significant NO is produced from product produced by diffusion burning has caused some doubt about the validity of using only Zeldovich kinetics and not including other more complex reactions. However the good agreement shown here and in many other comparisons indicates that a more complex kinetics model may not be needed.

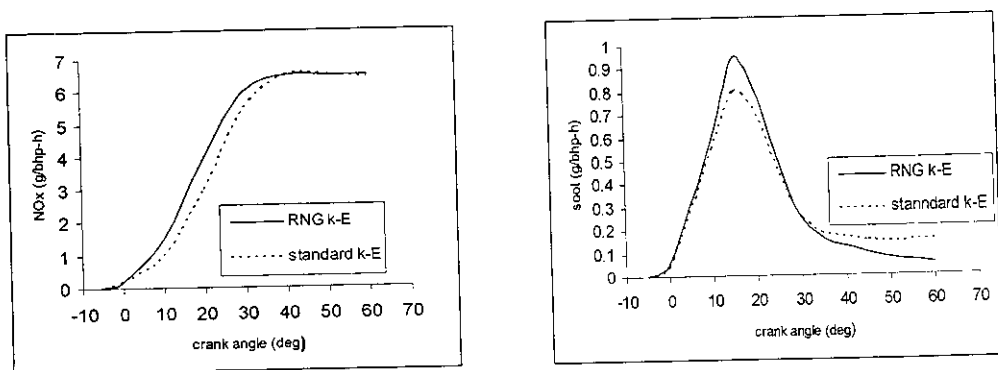


FIG 5.5 CRANK ANGLE VS NO_x AND SOOT

More fundamentally based models show promise to work well, but are not yet fully validated. The figure 5.5 shows the soot history corresponding to the engine conditions. Note that the change in turbulence model produced higher soot production but also more oxidation from previous experimental

Chapter 6

Modeling of IC Engine

6.1 PROBLEM DEFINITION

The combustion system considered in this study is 4-stroke compression ignition engine. The individual system components are shown in Appendix. The objective is to simulate the combustion in the combustion chamber and to predict the amount of exhaust gas composition for different type of air/fuel mixture. In this study the boundary conditions are more detailed (as discussed further in this section) and therefore are expected to provide more accurate results.

It is required that from the CFD solution the following be determined:

- The flow behaviour in the intake, combustion chamber, exhausts.
- Composition of exhaust gas emission.

TABLE 6.1

ENGINE GENERAL SPECIFICATIONS

Type of Engine	Four Stroke CI Engine
Type of Injection	Direct Injection
Fuel	High Speed Diesel
Bore X Stroke	80 mm X 110 mm
Compression Ratio	18: 1
Rated Power	4.25 KW (6 H.P)
Engine Speed	1500 rpm

TABLE 6.2

THE VALVE TIMING SPECIFICATION OF DI ENGINE

Inlet Valve opens	6° before TDC
Inlet Valve closes	12° after BDC
Fuel Injection begins	18° before TDC
Fuel Injection ends	20° after TDC
Exhaust Valve opens	45° before BDC
Exhaust Valve closes	6° after TDC

TABLE 6.3**INLET VALVE SPECIFICATION OF DI ENGINE**

Base diameter	36.694 mm
Throat diameter	10.2 mm
Valve lift	8.3 mm
Valve height	165 mm

TABLE 6.4**EXHAUST VALVE SPECIFICATION OF DI ENGINE**

Base diameter	37 mm
Throat diameter	11.06 mm
Valve lift	7.3 mm
Valve height	163 mm

TABLE 6.5**THE INJECTOR SPECIFICATION OF DI ENGINE**

Number of hole	1
Nozzle hole diameter	0.32 mm
Nozzle hole length	1.232 mm
Nozzle maximum valve lift	1.4 mm
Injection pressure	137.293 bars
Nozzle hole coefficient discharge	0.66
Ambient pressure	1 atm
Ambient Temperature	300° K

6.2 GEOMETRY AND GRID GENERATION

The gambit is the pre-processor used to create the geometry and the grid. Both triangular and quad meshes were created, in total over 15 grids of varying dimension and element types. The view of the grid can be seen in the figure 6.1 shown below. The grid was then imported into the Computational Fluid Dynamics (CFD) package, FLUENT for case set up and solving for the flow.

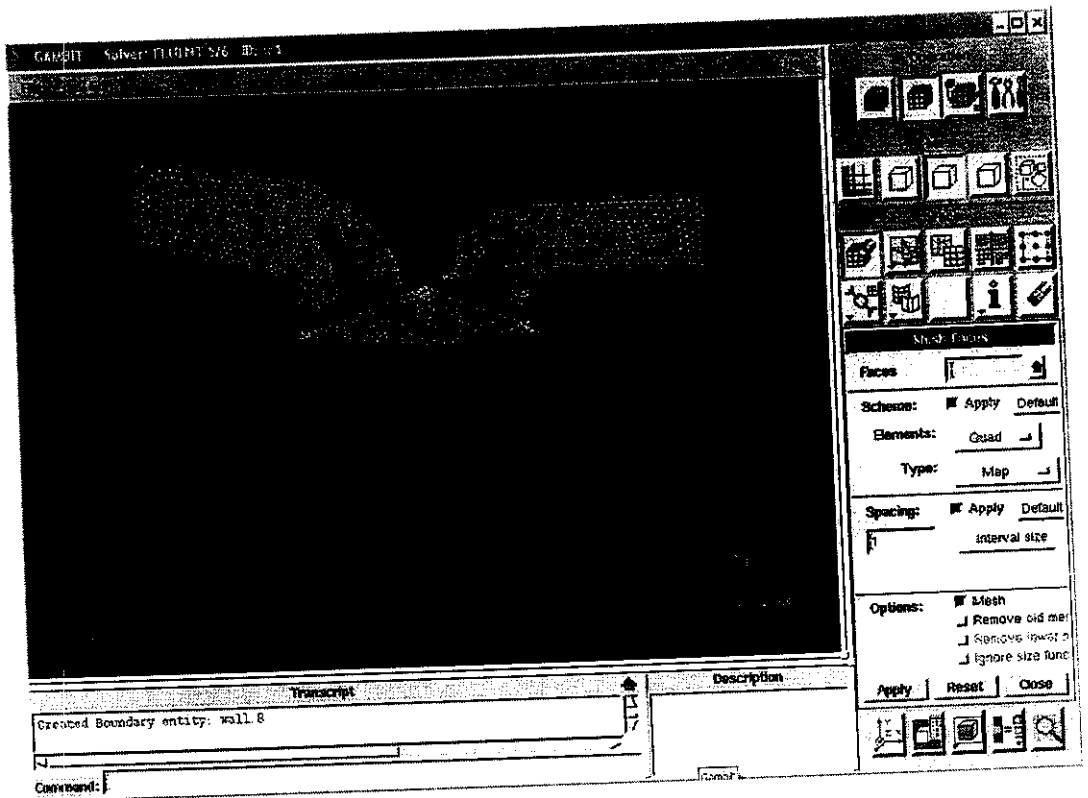


FIG 6.1 MODEL AND GRID GENERATION

6.3 BOUNDARY CONDITION

Two pressure boundaries were specified at the inlet and outlet of the intake and exhaust manifold with a specified pressure for the initial steady-state CFD simulation. The pressure inlet boundary is used to represent atmospheric pressure. At the pressure outlet boundary, a required pressure is specified to initiate intake flow. This is shown in the figure 6.2.

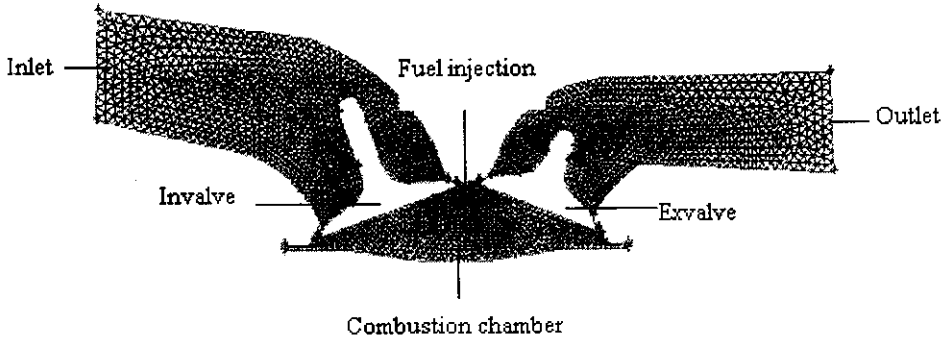
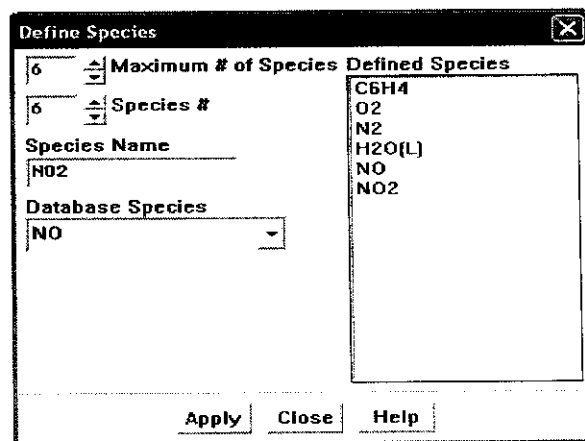


FIG 6.2 VARIOUS COMPONENTS IN THE MODEL

6.4 pre-PDF PREPROCESSOR

The mixture-fraction/PDF modeling approach allows you to model Non-premixed turbulent combustion by solving a transport equation for a single conserved scalar, the mixture fraction. Multiple chemical species is included in the problem definition and their concentrations will be derived from the predicted mixture fraction using the assumption of equilibrium chemistry. Property data for the species are accessed through a chemical database.

When you use the mixture-fraction/PDF model, you begin by preparing a PDF file with the preprocessor, PrePDF. The PDF file contains tables relating species concentrations and temperatures to the mixture fraction. The tables shown in the figure 6.3 are used by FLUENT to obtain these scalars during the solution procedure.



6.5 SETUP AND SOLUTION

The grid was then imported into the Computational Fluid Dynamics (CFD) package, FLUENT for case set up and solving.

Model

This process involves enabling the time standard calculation, as dynamic mesh simulations currently work only with the 1st-order time advancement. Multiple species model is used, since the simulation involves combustion, you will track the amount of burned 'residual' gas in the combustion chamber.

Materials

The types of material and chemical formula are specified in material panel. The material used here are air and pdf- mixture, property such as density, thermal conductivity and viscosity for the material are also specified in the same panel list.

Mesh Motion

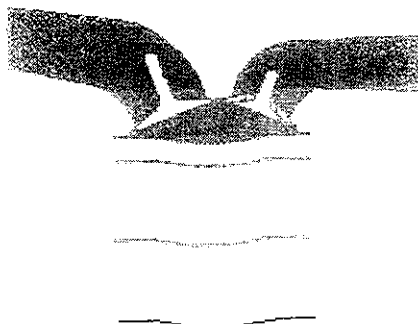
The mesh motion show additional inputs of in-cylinder, remeshing and Layering.

The Remeshing parameter is used to display.

- Set the Minimum Cell Volume to $1.0e-7$ m³.
- Set the Maximum Cell Volume to $3.0e-6$ m³.

The layering parameter is used to display

- Split factor to 0.4
- Collapse factor to 0.04
- Enable the constant ratio



The in-cylinder is used to specify the various other parameters,

- Crank Shaft Speed to 1500 rpm.
- Starting Crank Angle to 0 degrees.
- Piston Stroke to 80 mm and Connecting Rod Length to 140 mm.

The mesh is currently at the top dead center (TDC) position with both valves Closed. Later, you will move the mesh to the starting position which is near the intake valve opening. The figure 6.4 shows the movement of the mesh.

Injection point

The flow of liquid fuel droplets is defined by the initial conditions that describe the droplets as they enter the air stream.

TABLE 6.6
INITIAL CONDITION UNDER POINT PROPERTY

	First point	Last point
X-position	0.0313744845	0.0313744834
Y-position	0.10144066	0.10144066
X-velocity	100	100
Y-velocity	0	57.7
diameter	100	100
temperature	303	303
Flow rate	2.0E-4	2.0E-4

Solution

Solution limits are useful from preventing the intermediate solution from oscillating and prevents solver divergence. This is especially critical for times when large changes occur, such as when a valve begins to open. The solution limits should not be too restrictive to affect the converged solution at the end of a time step. If solution limits are reached, FLUENT reports this to the console.

Chapter 7

Result and discussion

7.1 RESULT

The simulation performed in this section will be used mainly for comparison purposes as the complexity of the simulations increases. Therefore only the mass flow rate and emission of combustion are discussed.

The figures in the following section illustrate burned gas at various crank angle position.

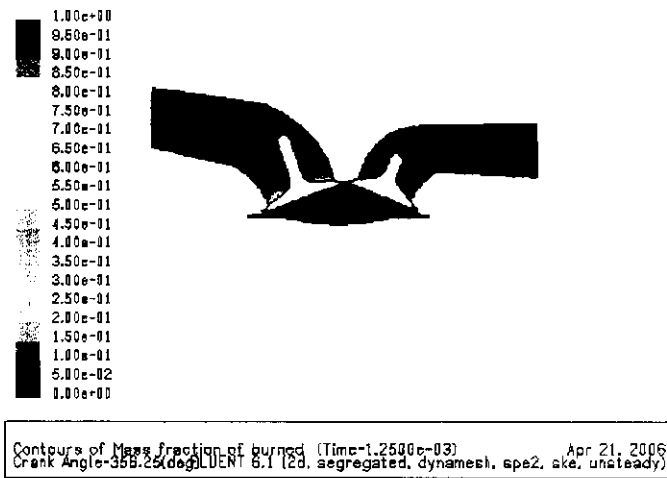


FIG 7.1 MASS FRACTION OF BURNED AT STARTING OF SUCTION STROKE

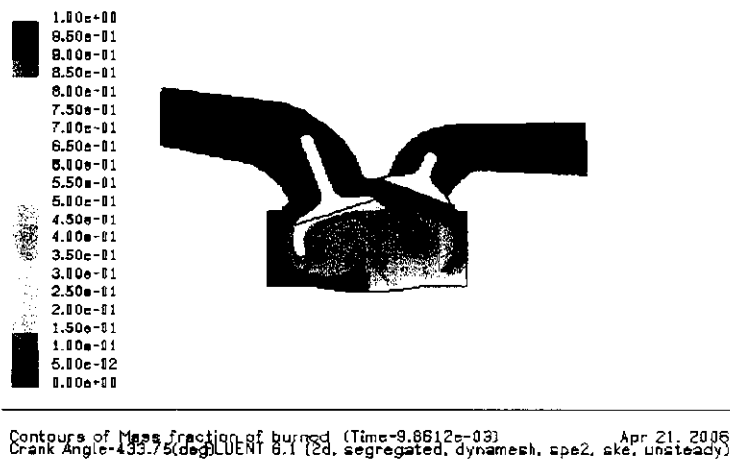
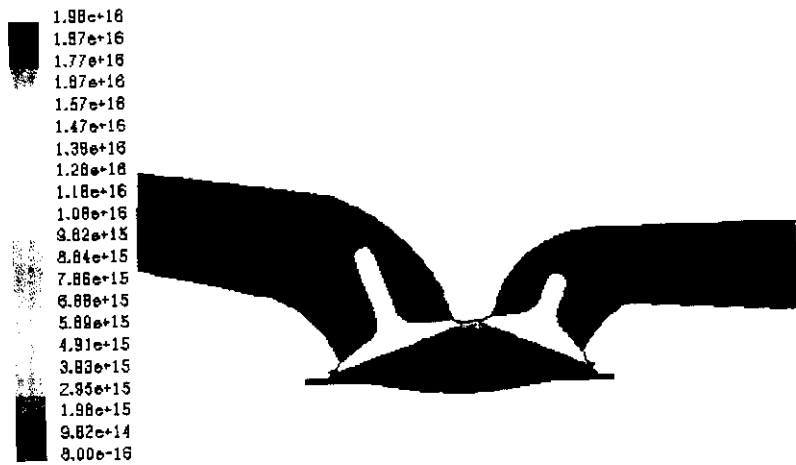
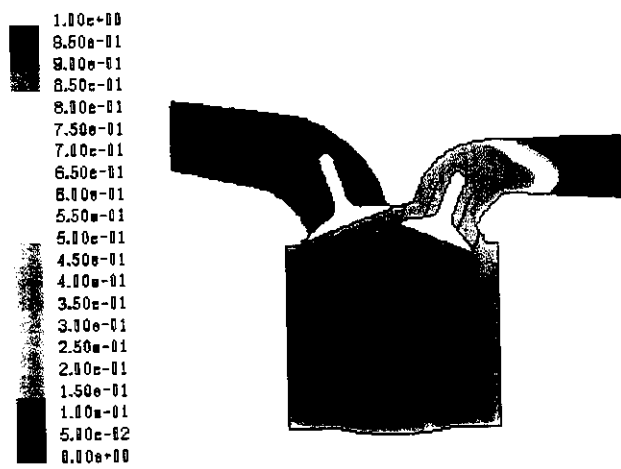


FIG 7.2 MASS FRACTION OF BURNED AT ANGLE OF 430⁰



Contours of Turbulent Kinetic Energy [k] (m2/s2) Apr 22, 2006
Crank Angle=389.167.93(deg) FLOWENT 6.1 [2d, segregated, dynamesh, pdf11, ske]

FIG 7.3 TURBULENCE KINETIC ENERGY



Contours of Mass fraction of burned (Time=6.6862e-02) Apr 21, 2006
Crank Angle=946.75(deg) FLOWENT 6.1 [2d, segregated, dynamesh, spe2, ske, unsteady]

FIG 7.4 MASS FRACTION OF BURNED AT STARTING OF EXHAUST STROKE

Each stroke in the simulation shows formation of burned gas. From the figure (7.1), (7.2), (7.3), (7.4) above we can able to predict that burning of gas take place immediately after air enters into the chamber due to presence of high temperature.

The figures in the following section illustrate mass fraction of emission from the combustion process at the exhaust valve.

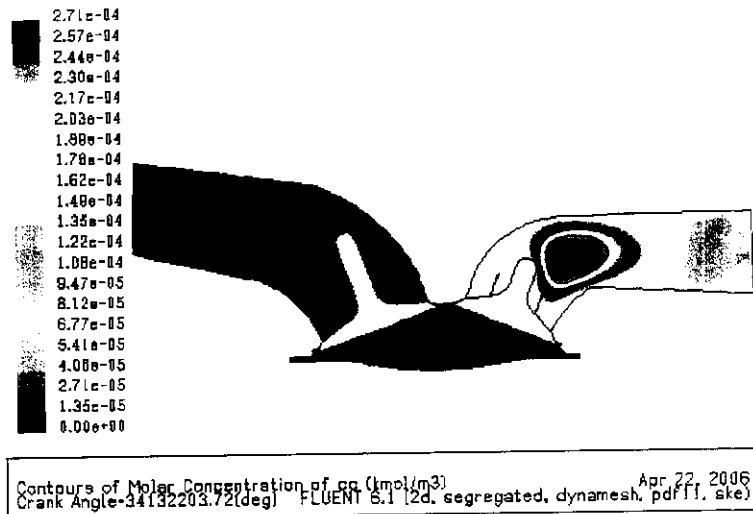


FIG 7.5 MOLE CONCENTRATION OF CO

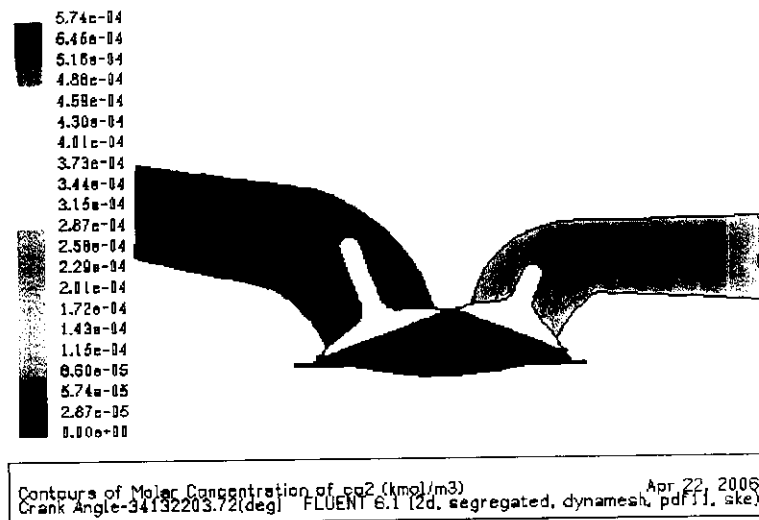
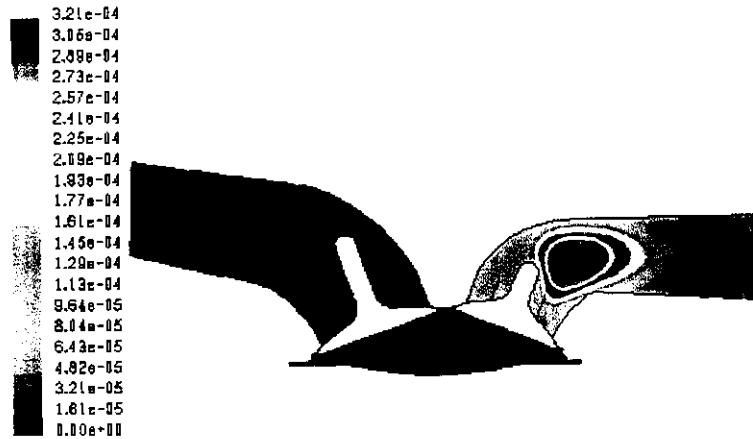
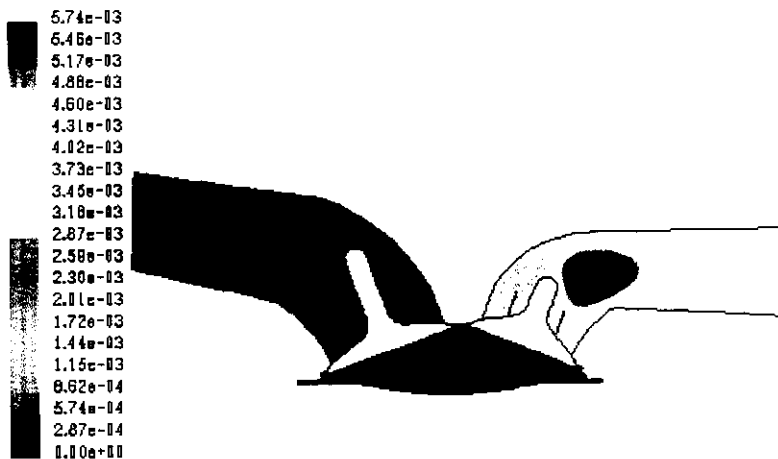


FIG 7.6 MOLE CONCENTRATION OF CO₂



Contours of Molar Concentration of h2 (kmol/m3) Apr 22, 2006
Crank Angle=34132203.72(deg) FLUENT 6.1 (2d, segregated, dynamesh, pdf11, ske)

FIG 7.7 MOLE CONCENTRATION OF H₂



Contours of Molar Concentration of n2 (kmol/m3) Apr 22, 2006
Crank Angle=34132203.72(deg) FLUENT 6.1 (2d, segregated, dynamesh, pdf11, ske)

FIG 7.8 MOLE CONCENTRATION OF N₂

The figures (7.5), (7.6), (7.7), (7.8) clearly show the emission of gases such as carbon-monoxide, carbon-dioxide, hydrogen, nitrogen, and oxygen. The amounts of emission are approximately predicted from the simulation. Among all the emission, the emission of NO_x is assumed to be high.

Chapter 8

Conclusion

The non-premixed combustion process in a compression ignition engine has been simulated cycle by cycle using a FLUENT code. The combustion model used for the calculations has been tested against simulation results under a particular engine conditions. This study leads to the conclusion that the combustion model tested shows encouraging results.

The investigations have revealed that during the combustion period the wall heat flux varies substantially in space and time, due to the transient nature of the flame propagation. In particular, during the early stages of flame, the heat flux undergoes rapid increases. These variations can have important consequences for the design of components, especially the piston, which in the Diesel engine are subject to particularly high pressure and thermal loads. Also the flame propagation is not uniform; this may lead to improper combustion. This can be reduced by changing the valve timing diagram, and the timing of injection of fuel.

The various emissions such as Carbon-monoxide, Carbon-dioxide, water, Nitrogen, Nitrous oxide are predicted using the CFD code. The predicted value shows some huge amount of NO_x emission, which results the engine is not running at maximum efficiency. Therefore some design modification has to be considered so that we can reduce the amount of emission NO_x. Some of the emissions are compared with the theoretical chemical equilibrium.

References

1. Blair, PG (1999), Design and Simulation of Four-stroke Engines, *Society of Automotive Engineers, Inc.* Warrendale, Pa.
2. Borman, G and Nishiwakik, K, Internal Combustion Engine heat transfer, *Progress in energy and combustion Science*, pp.1-46
3. Engström, J, Kaminski, G & Magnusson, I (1998), Experimental Investigations of Flow and Temperature Fields in an CI Engine and Comparison with Numerical Analysis, *Proceedings of International Fuels & Lubricants Meeting & Exposition*, Toronto, Canada.
4. Ferrari, G, Onorati, A, Piscaglia, F, Fluid Dynamic Simulation Of A Six-Cylinder S.I Engine With Secondary Air Injection In The Exhaust After-Treatment System, *Society of Automotive engineers, Inc*
5. Heywood, JB. (1992), *Internal Combustion Engine Fundamentals. McGraw-Hill International*, Edition 3, New York
6. Holger peters, Ralph Worret, (2001), Numerical Analysis of the Combustion Process in Spark-Ignition Engine, *The Fifth International Symposium on Diagnostics and Modeling of Combustion in IC Engines*.
7. Ismail B. Celik, (1999), Introductory Turbulence Modeling, *West Virginia University, Mechanical Engineering Dept.* Morgantown, pp.1-40
8. Jeyachandran, K and Manoharan, N (2000), Computer simulation of a 4 stroke Adiabatic Diesel Engine, *Narosa Publishing House*, New Delhi, India.
9. Kirkpatrick, Allan, WillsonBryan, (1998), Computational and Experimentation On The Web With Application to Internal Combustion Engines, *Journal of Engineering Education*
10. Mayer, K.; Spicher, U. (2000) Optical Investigations on Combustion in a DI Diesel Engine with and Endoscopes System and the Two Color Method, *ASME S an Antonio*.
11. Roger A. Strehlow, (1984), Combustion Fundamentals, *McGraw- Hill International*, New York, pp.252-364
12. Stephen, R.Turns, (2000), An Introduction to Combustion, *McGraw-hill international, New York*, pp. 423-450
13. Subramaniyam, S, Ganesan, V, Srinivasa Rao, p, Sampth, S (1988), Experimental Investigation on the turbulent flow inside the cylinder of a Diesel Engine, *16th National conference Fluid Mechanics and Fluid power*.
14. Smith, PH & Morrison, JC (1968), The Scientific Design of Exhaust and Intake Systems, *Second Edition, G. T. Foulis & co, LTD.* London.
15. Trigui, N, Griaznov, V Affes, H and Smith, D (1999), CFD Based Shape Optimization of IC Engine, *Journal of Engineering Education*.